

# Controlled Agentic Planning & Reasoning for Mechanism Synthesis

João Pedro Gandarela<sup>1,2</sup> Thiago Rios<sup>3</sup> Stefan Menzel<sup>3</sup> André Freitas<sup>1,4,5</sup>

<sup>1</sup>Idiap Research Institute, Switzerland

<sup>2</sup>École Polytechnique Fédérale de Lausanne (EPFL), Switzerland

<sup>3</sup>Honda Research Institute Europe, Germany

<sup>4</sup>Department of Computer Science, University of Manchester, UK

<sup>5</sup>National Biomarker Centre, CRUK-MI, University of Manchester, UK

firstname.lastname@idiap.ch, joao.gandareladesouza@epfl.ch

firstname.lastname@honda-ri.de, andre.freitas@manchester.ac.uk

## Abstract

This work presents a dual-agent Large Language Model (LLM)-based reasoning framework for automated planar mechanism synthesis that tightly couples linguistic specification with symbolic representation and simulation. From a natural-language task description, the system composes symbolic constraints and equations, generates and parametrises simulation code, and iteratively refines designs via critic-driven feedback, including symbolic regression and geometric distance metrics, closing an actionable linguistic/symbolic optimisation loop. To evaluate the approach, we introduce MSynth, a benchmark of analytically defined planar trajectories. Empirically, critic feedback and iterative refinement yield large improvements (up to 90% on individual tasks) and statistically significant gains per the Wilcoxon signed-rank test. Symbolic-regression prompts provide deeper mechanistic insight primarily when paired with larger models or architectures with appropriate inductive biases (e.g., LRM).

## 1 Introduction

The combination of LLM-based reasoning with simulation environments (Fu et al., 2024; Bhat et al., 2024; ichter et al., 2023) represents a promising research stream for systematising and scaling-up quantitative analysis across areas such as Physics, systems biology and engineering. By interfacing linguistic/symbolic-level interpreters with simulation models, one can develop closed-loop systems where design hypotheses are continuously validated and refined based on dynamic feedback from simulation outputs (Wang et al., 2024; Rana et al., 2023).

The design and synthesis of planar mechanisms is an example of a problem space which requires the coordination of expert-level reasoning steps across different representational domains:

language-based, topological, equational, dynamic and geometric. Traditionally, engineers synthesise mechanisms by using kinematic diagram representations and topological graph-based methods, which provide structured search spaces for the application of conventional optimisation algorithms (García-Marina et al., 2020). Typically, the design of a mechanism is divided into two main phases: A conceptual phase and a dimensional synthesis phase (Fig. 1). In the conceptual phase, one defines the overall layout of the mechanism (number of links, number of joints and types of joints) based on the design requirements, e.g., the number of degrees of freedom (Tsai, 1999). Once the layout is fixed, in the dimensional synthesis phase, one defines geometric properties of the links and joints to enable the mechanism to perform a predefined task, which is typically to move the end effector through a predefined trajectory while sustaining mechanical loads (Romero et al., 2019). However, currently available methods for both conceptual design and dimensional synthesis require experienced users to select a solution from a set of enumerated conceptual designs, identify redundancies and overconstrained kinematic chains, as well as lack scalability with respect to the complexity of the end effector trajectory and target number of degrees of freedom.

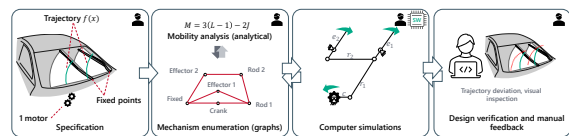


Figure 1: Example windshield-wiper synthesis workflow. Engineers first generate a candidate mechanism, use these to build simulations during a dimensional-synthesis step, and then iteratively refine topology and dimensions based on simulation performance until the design meets targets.

Recent advancements in machine learning (Vasilii

and Yannou, 2001; Sonntag et al., 2024), particularly LLMs, have inspired new directions in automated mechanism design. It has been shown that LLMs perform an initial level of linguistic interpretation, simulation code generation/parametrisation, thus making them potentially well-suited for addressing the basic reasoning required for mechanism synthesis. However, the reasoning mechanisms for supporting this synthesis remain largely informal, thus limiting the complexity and control of generated mechanisms. The main modelling challenge behind mechanism synthesis lies in the need to reason over and interpret non-linguistic data, e.g. trajectories, geometrical/dynamical properties together with natural language, code generation and equational/mathematical reasoning.

This paper addresses this gap *by providing the first end-to-end, well-formalised, cyclic refinement paradigm for mechanism synthesis reasoning*. At the centre of the proposed model is the decomposition of the formal components involved in the underlying mechanism synthesis reasoning process. The proposed framework is conceptualised across two functional clusters: a Designer Agent ( $\mathbb{D}a$ ) and a Critique Agent ( $\mathbb{C}a$ ) function. While  $\mathbb{D}a$  encapsulates the requirements interpretation, mechanism abstraction, mathematical framing, simulation generation and refinement of mechanism configurations,  $\mathbb{C}a$  provides a systematic mechanism to evaluate the generated mechanisms based on simulation outcomes, compliance to mechanical constraints and target properties. The iterative dialogue between these two agents creates a constructive feedback loop, wherein systematic design updates and targeted critique drive the convergence towards a mechanism that closely satisfies the specified target properties. These underlying functions, integrate the heterogeneous domains required to perform mechanistic reasoning. In summary, our contributions are:

**1.** We propose a mechanism synthesis reasoning framework (design-critique) that integrates LLM-driven design generation with simulation-based evaluation, critique and refinement. **2.** We formalize the underlying systematic design-critique reasoning process, defining an iterative refinement model which, given a set of mechanism requirements, can abstract, instantiate and refine over the mechanism states and properties. **3.** We demonstrate an efficient iterative optimization strategy that leverages a memory repository to capture and

build upon successful design strategies across iterations, ultimately minimizing the deviation between the target and generated trajectories. **4.** We introduce *MSynth*<sup>1</sup> a new benchmark for planar mechanism synthesis. **5.** We empirically analyse the impact of each reasoning component and contrast how different foundation LLM architectures compare in terms of design quality, convergence speed, and computational cost.

## 2 Proposed Method

The general goal of a planar mechanism design is to generate a mechanism  $Mech$  that moves an end effector through a target path, which is described as a set of points or an analytical curve. Given a set of analytical equations  $\mathcal{T}$  defining the desired trajectory, our proposed model automatically generates a mechanism configuration that yields a motion path  $\mathcal{G}$  that minimises the deviation with respect to the targeted trajectory and satisfies other design constraints (e.g., number of links).

During the design process, currently available design approaches typically represent mechanisms using graphs and analytical kinematics models. While these representations provide structured search spaces that enable traditional optimisation algorithms to explore candidate designs, they *require an expert-driven manual set-up and post-hoc analysis* (Figure 1). In contrast, we propose a neuro-symbolic (Nawaz et al., 2025; Wan et al., 2024) LLM-based reasoning paradigm which, starting from a natural language specification of the requirements, employs a code-based representation to specify mechanism components, connections, and parameters directly. This approach offers greater expressiveness in mechanism specification and yields a broader search space when compared to standard representations. To navigate the design space effectively, at the design phase, we leverage LLMs for supporting an abstract mechanistic reasoning over the mechanism requirements, interpreting mechanics background knowledge, and formalising a design hypothesis via code generation for a target simulator. Within the planar setting, the target mechanism entails a trajectory in the  $\mathbb{R}^2$  domain. Formally, let  $\pi_\theta$  denote a pre-trained LLM with parameters  $\theta$ . We iteratively sample mechanism designs  $\mathcal{F} = Mech : Mech \sim \pi_\theta$ , aiming to minimize the distance  $d$  between the target and

<sup>1</sup>anonymized

generated trajectories:

$$Mech^* = \arg \min_{\mathcal{M} \in Mech} d(\mathcal{T}, \mathcal{G}_{\mathcal{M}})$$

In order to optimise  $Mech^*$ , the proposed model formalises an iterative refinement workflow consisting of a Designer Agent ( $\mathbb{D}a$ ), which generates and refines candidate mechanisms, and a Critique Agent ( $\mathbb{C}a$ ), which evaluates the generated designs based on predefined constraints, simulation results, and historical performance data. The agents operate in a feedback loop, where the  $\mathbb{C}a$ 's evaluations guide the design refinements performed by the  $\mathbb{D}a$ . Hence, by leveraging both current performance metrics and inferred properties from past iterations, the feedback loop enables the continuous improvement of the designs, which potentially converge to optimal solutions. The following sections describe and formalise the underlying reasoning components that support this adaptive design process (Fig. 2). The overall procedure is formalised in Algorithm 1, which outlines the dual-agent loop of design generation, simulation, critique evaluation, and revision. The proposed model is packaged within *Mechanic*<sup>2</sup>, an adaptive solver for mechanism synthesis.

## 2.1 Designer Agent

The  $\mathbb{D}a$  concentrates the set of functions for the generation of the mechanism design. Given a mechanism specification  $\mathcal{M}(\theta)$ , Simulator  $Sim$ , Set of examples  $\mathcal{E}x$ , Target points along the end effector trajectory  $\mathcal{P}$ , and Analytical equation of the target path  $\mathcal{T}$  (to provide a closed-form objective against which deviations are measured), the  $\mathbb{D}a$  applies an evaluation function:

$$\mathbb{D}a(\mathcal{M}(\theta), Sim, \mathcal{E}x, \mathcal{P}, \mathcal{T}) \rightarrow Mech$$

Here, the  $\mathbb{D}a$  moves from a natural-language description of the task (the prompt and symbolic specs) to a mechanical hypothesis  $Mech$ , the instantiation of a mechanism under a simulator  $Sim$  that satisfies  $\mathcal{M}(\theta)$ , and ultimately targets a geometric trajectory in Cartesian ( $\mathbb{R}^2$ ) space. At each iteration  $t$  (to explore the search space efficiently while maintaining diversity), we sample a batch of  $b$  mechanism configurations  $F_t = \{f_i\}_{i=1}^b$ ,  $f_i \sim \mathbb{D}a(\cdot \mid p_t)$ , where  $p_t$  is the constructed prompt (Appendix E). Each candidate is validated via simulation in  $Sim$ , and those yielding errors are discarded to prevent ill-defined features from propagating into subsequent design iterations. Thus the

<sup>2</sup>anonymised

$\mathbb{D}a$  goes from: linguistic prompt  $\rightarrow$  mechanical candidate  $\rightarrow$  geometric/ $\mathbb{C}a$  validation  $\rightarrow$  refined prompt.

We structure the prompt in four abstraction stages, each adding a layer of guided inference control. First, a motion-profile alignment with the target analytical equations ensures the geometric trajectory faithfully follows the analytic specification. Next, an enforcement of structural constraints, such as naming the critical joint ‘‘target’’, to guarantee mechanical integrity and facilitate downstream parsing. Then, a systematic refinement via iterative feedback loops that embed linguistic guidance into each design iteration. Finally, a sequential code generation that preserves a clear, logical progression from prompt to executable model. These principles are materialised in a structured prompt composition, formalised as follows (see Appendix F for the complete instantiation):

We now formalise how the  $\mathbb{D}a$  integrates these abstractions. Each  $f_i$  injects a new reasoning layer:  $P_d = f_{Mem} \circ f_{Con} \circ f_{Ex} \circ f_{Sim}(\text{Input})$ , where each function  $f_i$  represents a distinct processing stage:  $f_{Sim}$ : Embeds Simulator documentation and mechanism descriptions;  $f_{Ex}$ : Contains concrete examples and reference models;  $f_{Mem}$ : Integrates memory containing previous designs and evaluations;  $f_{Con}$ : Applies key constraints (key points) and target analytical equations.

The  $\mathbb{D}a$  minimises the deviation (this is the geometric objective that closes the loop back to the analytic target  $\mathcal{T}$ ) from the target path defined by the function  $\mathcal{T}$ . The optimization objective can be formalized as  $\arg \min_i d(\mathcal{M}(\theta_i), \mathcal{T})$ , where  $d(\cdot, \cdot)$  represents a distance metric measuring the deviation from the target  $\mathcal{T}$  to the target path  $\mathcal{M}(\theta_i)$  at time step  $i$ . The  $\mathbb{D}a$  iteratively refines the mechanism parameters  $\theta$  through feedback-driven updates and leverages Symbolic Regression (SR) (Schmidt and Lipson, 2009; Petersen et al., 2021; Shojaee et al., 2025, 2023; Meidani et al., 2024) to extract expressions that guide the optimisation.

## 2.2 Critique Agent

This agent evaluates designs generated by the  $\mathbb{D}a$  across multiple dimensions and synthesises structured feedback to guide the iterative design refinement. Given a designed mechanism  $\mathcal{M}(\theta)$ , Simulator Output  $\mathcal{S}$ , Memory repository  $Mem$ , and Designer Response  $\mathcal{R}$  (to ground its critique in past

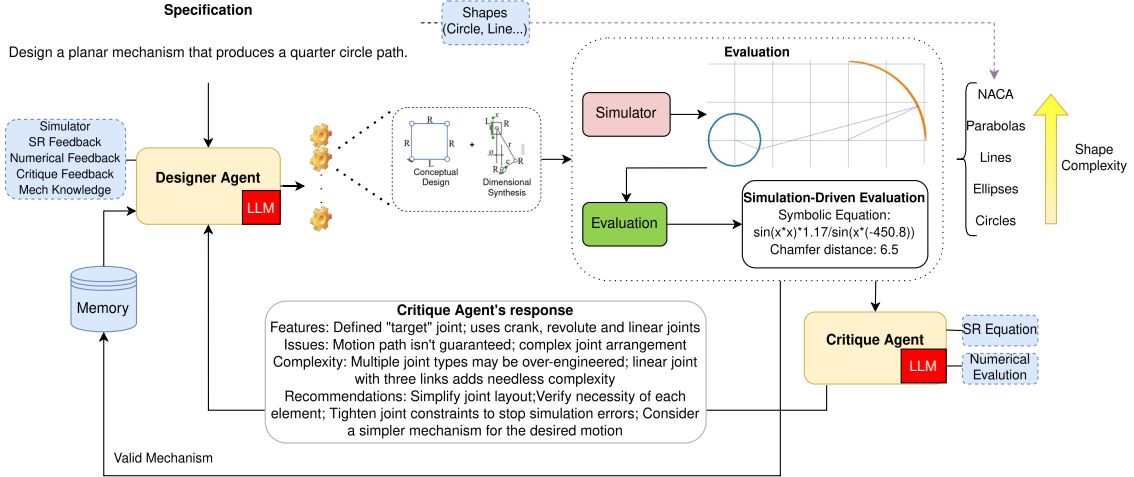


Figure 2: LLM-guided pipeline for synthesising planar mechanisms with a quarter-circle end-effector path: the  $\mathbb{D}a$  generates proposals using domain knowledge and memory; the simulator returns numeric metrics and a Symbolic Regression (SR) trajectory; the  $\mathbb{C}a$  provides recommendations; simulator+critique feedback loop back to the DA for iterative refinement until a valid design emerges.

designs, fresh simulation data, and the designer’s own rationale), the  $\mathbb{C}a$  applies an evaluation function:  $\mathbb{C}a(\mathcal{M}(\theta), \mathcal{S}, \text{Mem}, \mathcal{R}) \rightarrow \mathbb{F}$ .

Here, the  $\mathbb{C}a$  maps the geometric output of the simulator back into a linguistic analysis space, producing feedback  $\mathbb{F}$  that will inform the next iteration of mechanism hypotheses. The  $\mathbb{C}a$  assessment incorporates specialised knowledge on mechanical design principles and constraints, kinematics simulation and performance analysis (so that feedback reflects not just form but function), historical context based on previous successful designs, structural complexity and optimisation potential (Appendix F). *Together, these layers abstract and contextualise the numerical simulation output to inform the next design cycle.*

We decompose the  $\mathbb{D}a$  into four abstraction functions, each mapping to properties of the current design state back into linguistic guidance: (1) **Correctness Assessment**: Adherence to constraints and functionality. (2) **Error Identification**: Structural or functional issues; (3) **Complexity Analysis**: Structural efficiency and design elegance. (4) **Refinement Suggestions**: Actionable design improvements.

We now formalise the  $\mathbb{C}a$ ’s reasoning pipeline, showing how it reconstructs the design story from multiple abstraction layers (Appendix F):

$$\mathcal{P}_c = f_{\text{mem}} \circ f_{\text{sim}} \circ f_{\text{ex}} \circ f_{\text{des}}(I),$$

$f_{\text{des}}$ : ingests the linguistic output of  $\mathbb{D}a$  as raw cri-

tique material.  $f_{\text{sim}}$ : aligns feedback with fresh geometric/mathematical (SR)/simulation data.  $f_{\text{ex}}$ : draws on exemplar critiques to standardize style and depth.  $f_{\text{mem}}$ : grounds each evaluation in historical context for consistency.

### Symbolic regression as trajectory surrogate

Converting a numerical trajectory into a compact symbolic form yields a concise, meaningful abstraction that both human designers and automated critics can manipulate as a shared language. SR provides an abstraction layer that changes the nature of reasoning about mechanism behaviour. Instead of treating simulation output as uninterpreted sensory data, our method elevates it to a compact symbolic description that can be composed, constrained and communicated. We use SR to produce compact, interpretable surrogates  $S$  of simulator-generated trajectories  $\mathcal{G}$ .

Let  $\mathcal{G}$  be the simulator trace and  $S$  a symbolic surrogate. We fit SR by minimising loss:  $\mathcal{L}(S) = d(\mathcal{G}, \mathcal{T})$ , where  $d(\cdot, \cdot)$  is the trajectory error. Rather than reasoning over raw samples, the LLM reasons over higher-level expressions that expose functional motifs (periodicity, monotonic segments). This abstraction acts as shared semantics, a common language for the  $\mathbb{D}a$ , the  $\mathbb{C}a$  and human reviewers, improving transparency and enabling principled critique, validation and transfer of ideas across iterations. Viewed this way, the numeric→symbolic transformation is not just data summarisation: it is a change in the representa-

tional substrate that enables higher-order reasoning, and more interpretable design refinement.

### 2.3 Revision

The revision function operates as a feedback-mediated transformation system that enables iterative refinement of planar mechanisms. Given a Designer Response  $\mathcal{D}_r$ , Critique Response  $\mathcal{C}_r$ , a Simulator Output  $\mathcal{S}$ , and a Memory Repository  $\mathcal{Mem}$ , the revision process applies a transformation function:  $\mathbb{R}_p(\mathcal{D}_r, \mathcal{C}_r, \mathcal{S}, \mathcal{Mem}) \rightarrow \mathcal{D}'_r$ .

Here, the revision function bridges from the linguistic artefacts of the designer and critic back into a mechanical proposal ( $\mathcal{D}'_r$ ), ready for geometric validation in the next loop, where:  $\mathbb{R}_p$ : Revision function responsible for mechanism refinement;  $\mathcal{D}_r$ : Designer Response containing the current mechanism implementation;  $\mathcal{C}_r$ : Critique Response providing structured feedback;  $\mathcal{S}$ : Simulator Output containing execution traces and validation results;  $\mathcal{Mem}$ : Memory Repository storing previous designs and outcomes;  $\mathcal{D}'_r$ : Refined Designer Response with improved implementation.

At each refinement iteration  $t$ , we generate a revised mechanism  $\mathcal{D}'_{r,t}$  based on the previous implementation and feedback:

$$\mathcal{D}'_{r,t} = \mathbb{R}_p(\mathcal{D}_{r,t-1}, \mathcal{C}_{r,t-1}, \mathcal{S}_{t-1}, \mathcal{Mem}_{t-1})$$

*This iterative rule encapsulates how the system cycles through linguistic feedback, mechanical transformation, and geometric re-evaluation.*

We codify three constraint checks, each ensuring the revision stays true to its linguistic instructions, mechanical fidelity, and geometric performance: **(i) Feedback Adherence:** The revision incorporates and addresses the provided critique:  $\forall f \in \mathcal{C}_{r,t-1}, \exists m \in \mathcal{D}'_{r,t} : \text{Addresses}(m, f) = 1$  **(ii) Simulation Consistency:** The revised mechanism aligns with physical simulation principles:  $\mathcal{V}(\mathcal{M}(\theta)'_{r,t}, \mathcal{S}_{t-1}) = 1$ . **(iii) Efficiency:** The revision eliminates redundancy while maintaining functional correctness:  $\text{Complexity}(\mathcal{M}(\theta)'_{r,t}) \leq \text{Complexity}(\mathcal{M}(\theta)_{r,t-1})$ , subject to  $d(\mathcal{D}'_{r,t}, \mathcal{T}) \leq d(\mathcal{D}_{r,t-1}, \mathcal{T})$ .

We materialise the revision function's prompt, layering linguistic inputs through mechanical checks and geometric validation (Appendix G):

$$\mathcal{P}_r = f_{\text{mem}} \circ f_{\text{sim}} \circ f_{\text{crit}} \circ f_{\text{des}}(\text{Input})$$

The first,  $f_{\text{des}}$ , incorporates the current  $\mathbb{D}a$  Response (to re-ingest the designer's latest implementation as the starting point). Next,  $f_{\text{crit}}$  applies structured critique from the  $\mathcal{C}a$  (to inject targeted, linguistic feedback into the revision prompt). Then,  $f_{\text{sim}}$  integrates empirical validation via simulation outcomes (to align proposed changes with up-to-date geometric/SR simulation results). Finally,  $f_{\text{mem}}$  leverages historical context from successful past designs (to recall proven patterns and avoid repeating mistakes).

The ultimate objective of the revision function is to minimise the discrepancy between the target trajectory and the mechanism-generated path. The process terminates when either the distance falls below an acceptable threshold  $\epsilon$  or the maximum number of revision iterations  $R_{\text{max}}$  is reached:  $d(\mathcal{M}(\theta)'_{r,t}, \mathcal{T}) \leq \epsilon$  or  $t \geq R_{\text{max}}$ .

### 2.4 Memory

The optimisation framework incorporates a memory system that captures and leverages previously validated mechanisms. In the optimisation process, the memory represents a structured repository of previously validated mechanisms. Formally: Let  $M_t = \{m_1, m_2, \dots, m_n\}$  denote the set of stored mechanisms at iteration  $t$ . A mechanism  $m_i$  is stored only if it satisfies the execution criterion:  $\mathcal{V}(m_i) = 1$ , where  $\mathcal{V}(m_i)$  is a validity function. Retrieval follows a selection function:

$$m_{\text{retrieved}} = \arg \min_{m_i \in M_t} d(m_i, m_{\text{target}}),$$

where  $d(\cdot, \cdot)$  represents a predefined distance metric. Memory within this framework consists exclusively of mechanisms that executed successfully in the simulation environment. This selective storage approach ensures the validity preservation across the mechanism repository, improves the computational efficiency through elimination of invalid designs, and favours the convergence of the design refinement via retention of proven designs. The storage increases proportionally with iterations, creating a progressively richer knowledge base that guides subsequent iterations.

**Retrieval Methodology.** The memory retrieval implements a proximity-based selection strategy: *1. Retrieval Criterion:* Mechanisms are prioritised based on their closeness to the current design objectives and *2. Multi-Exemplar Scenario:* When multiple examples are needed, the system retrieves

the top- $k$  mechanisms with the smallest distances, where  $k$  corresponds to the number of requested examples. Through the alignment of retrieved designs with current objectives, the memory component facilitates the transfer of successful principles from past iterations to new designs by continuously adapting and leveraging experience throughout the optimisation process.

### 3 Empirical Analysis

In this section, we present an empirical analysis to evaluate the mechanistic synthesis framework in an automated planar mechanism design scenario. The study aims to address the following research questions: **RQ1:** How does cyclic refinement affect the depth and precision of the search process in automated mechanism synthesis? **RQ2:** In what ways do symbolic representation features modulate the exploration-exploitation trade-off during design iteration? **RQ3:** How do different foundation LLM architectures compare in terms of design quality, convergence speed, and computational cost? **RQ4:** What are the distinct contributions of individual system components (e.g., memory,  $\mathcal{C}a$ ) to overall performance? **RQ5:** To what extent does integrating mechanistic knowledge accelerate systematic exploration and improve solution quality when employing large-scale LLMs?

**Experimental Setup.** To support the evaluation, we build a synthetic dataset which evaluates mechanism generation across a set of trajectories which are analytically defined, including elliptical, lemniscate, and complex polynomial paths, parametrised by increasing geometric complexity (the set of analytical shapes is defined in Appendix D). Each iteration samples 3 mechanisms from  $\mathbb{D}a$  (temperature = 0.8). These settings are designed to stress-test the dual-agent loop under controlled conditions. We set the  $R_{\max} = 20$  and  $\epsilon = 0.05$ . Simulation and analysis use PyLinkage and PySR (Farajallah, 2024; Cranmer, 2023). Finally, we applied the Iterative Closest Point (ICP) algorithm, using the implementation by (Drakoulis, 2023; Lu and Milios, 1997), to align the simulated and measured point clouds and thus refine the end-effector pose. The overall performance of the system is quantified based on both the Chamfer distance ( $d_{\text{Chamfer}}$ ) for geometric fidelity and the number of iterations ( $t_{\text{iter}}$ ) for efficiency.

**Interventions.** We ran a full-factorial abla-

tion to quantify the contribution of each component. The factors were: (i) **LLM**  $\in$  {Llama, Gemma, Qwen}; (ii) **Shape** (all shapes used in the study); (iii) **#Examples per task** ( $\#Ex \in \{2, 3\}$ ); (iv) **Memory (Mem)**  $\in \{0, 2\}$ , where 0 means memory retrieval is disabled; (v) **CA feedback (Fdbk)**  $\in \{\text{No}, \text{Yes}\}$ ; and (vi) **Symbolic-feedback (SFB)**  $\in \{\text{No}, \text{Yes}\}$ . Every combination of these levels was executed (LLM  $\times$  Shape  $\times$  #Ex  $\times$  Mem  $\times$  Fdbk  $\times$  SFB). The full results table is provided in Appendix K.

**Dataset.** We evaluate our approach on a set  $S$  of target trajectories based on six analytic planar curves: circles, ellipses, lines, parabolas, Lemniscates of Bernoulli ( $\infty$ ) (LB), and NACA four-digit airfoils (Jacobs et al., 1933; Abbott and Von Doenhoff, 2012), each parameterised by standard formulae. By measuring mean Chamfer distance, we observe a progression of trajectories of increasing complexity: NACA airfoils (easiest), then circles, ellipses, lines, LB, and finally parabolas (hardest). For each shape class, we generate 5 random instances by sampling shape parameters uniformly over their valid ranges, then draw  $n \in \{4\}$  points along the curve to form the target motion profile. More details on the dataset are provided in Appendix D and H.

**Evaluation Metrics.** Evaluation is performed using a composition of metrics *Chamfer Distance* and *Semantic success*. Trajectories are normalised under ICP. We define *Semantic success* as a binary indicator: a generated mechanism parses and executes in the simulator without parse/compile/runtime errors (see Appendix C).

#### 3.1 Results

**The proposed mechanistic synthesis reasoning model delivers geometric outcomes via a linguistic/symbolic interpretation.** Regarding **RQ1**, the proposed model allows mechanistic synthesis reasoning to be delivered by the systematic composition of linguistic specification, abstraction, simulation code generation, simulator evaluation, and repeated critique-driven refinement. While mechanism synthesis is an essentially dynamical/geometrical problem, it can be steered in a linguistic/symbolic form by the functional decomposition outlined in Sections 2.1, 2.2, and 2.3, which converges towards the desired geometric outcome. Initially, iterations without the critique feedback, explored broad regions (e.g.,

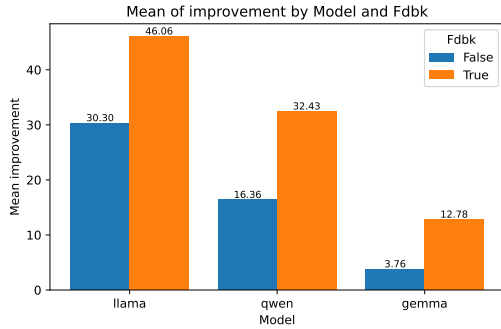


Figure 3: Average percentage improvement in Chamfer distance when comparing runs with feedback (Fdbk) versus without feedback. Incorporating feedback yields substantial gains, with the largest uplift observed for Llama3.3:70Bs (from 30% to 46%), demonstrating that feedback consistently enhances performance.

Llama3.3:70B: 12.537→2.673 Gemma3:12B: 8.826→6.288; Qwen3:4B: 1.893→1.111) up to 77.1%. Subsequent feedback-driven cycles exploit bigger gains and lower distances, yielding up to 49.9% Chamfer reduction for Gemma3:12B (2.021→0.997) and up to 90% for Llama3.3:70B (circle: 12.239→1.466).

**Feedback (critique) is the most impactful component across models.** Specifically, Gemma’s semantic success increased from 17.26% without feedback to 32.48% with feedback, an absolute gain of 15.22 percentage points (an  $\approx 88.2\%$  relative improvement). Llama’s semantic success rose from 53.02% to 62.43% with feedback, while Qwen showed a modest improvement from 42.13% to 42.69%. Additionally, providing feedback also increased the number of refinement rounds (mean rounds with feedback vs. without: Llama 11.943 vs 9.095; Gemma 12.483 vs 8.641; Qwen 11.817 vs 10.465), but yielded lower Chamfer distances. A paired Wilcoxon signed-rank test on the Chamfer distances showed a statistically significant difference between conditions, indicating that feedback, by enabling more iterative reasoning and steering the optimisation trajectory through symbolic representations, improves geometric fidelity. Fig. 3 shows that adding  $\mathbb{C}a$  feedback boosts final Chamfer gains across all three model families.

**Equational prompts affect large-scale models and Large Reasoning Model (LRM).** To evaluate the effect of SR (with Fdbk) against Fdbk without SR on performance, we compared results across all conditions and then examined the re-

sults. At the top-level analysis, the group using SR with feedback demonstrated a lower mean outcome (140.00) compared to the group without SR (148.50). The difference of  $\approx 8.5$  indicates that incorporating SR with feedback led to an improvement. When restricting the analysis to  $Mem = 2$ , this trend remained evident. (SR+Fdbk) again showed a lower mean than no SR, yielding a difference of  $\approx 6.94$ . This consistency across both the global and memory-controlled subsets strengthens the conclusion that SR contributes to reducing the measured outcome. A finer-grained shape-level comparison ( $Mem = 2$ ) further highlights the impact. Across most of the shape categories, SR+Fdbk yielded lower means compared to no SR. The reductions varied in magnitude. The largest reduction occurred for Parabola  $\approx 33.78$ ; Moderate reductions were observed for Ellipse ( $\approx 0.31$ ), LB ( $\approx 0.27$ ), and Naca ( $\approx 0.11$ ). Finally, SFB without feedback still yielded improvements for specific shapes (Circle and Ellipse). This indicates the benefits of SR+Fdbk and a shape-specific utility.

**Architecture and scale play a significant role in design quality.** In response to **RQ3**, we can notice that the Model-family and scale effects. Across the evaluated shapes, model family and training regime were far more predictive of performance than raw parameter count. In particular, the LRM-style model Qwen achieved the best aggregate minimisation largely driven by its superior performance on the Parabola task, whereas the dense Llama excelled on the other shapes (Circle, Ellipse, Line). For example, averaged over conditions the Parabola means were Qwen = 833.0944, Llama = 845.9883, and Gemma = 883.7850, while for the other shapes Llama attained the lowest means (Circle = 5.0016, Ellipse = 4.0585, Line = 3.5384). On Naca and LB, the models were much closer (Naca  $\approx 1.13$  for both Qwen and Llama; lb  $\approx 8.1$ -8.2), but Gemma was uniformly higher (further) across these shape categories. All models benefit from the combination of SFB and external feedback, but the magnitude of this benefit varies by architecture: Qwen exhibits the largest absolute improvements under SFB+feedback, Llama shows moderate gains, and Gemma the smallest. More generally, the advantage of the small LRM on Parabola demonstrates that the correct inductive biases and training regimen can make a compact model outperform much larger dense models on specific tasks.

### Semantic success rates (effect of feedback)

Feedback substantially increases semantic success for all architectures. Measured success rates rose from 49.74% to 73.69% for Llama, from 19.33% to 35.95% for Gemma, and from 39.25 to 48.73% for Qwen. Thus, while Llama attains the highest absolute success with feedback, Gemma shows the largest proportional improvement  $\approx 46\%$ ; Qwen improves moderately. These results underscore that feedback is a reliable lever to improve semantic performance across architectures, although the baseline competence and the magnitude of the gain depend on the model family.

### Memory and exemplars exhibit model-specific effects.

Memory and example-budget effects depend systematically on both architecture and scale: Qwen (LRM), a compact model, benefits consistently and substantially from increasing memory (Mem 0  $\rightarrow$  2), with aggregate means falling by  $\approx 11.6$  at numEx= 2 (150.498  $\rightarrow$  138.882,  $\Delta \approx -11.62$ ) and by  $\approx 11.4$  at numEx= 3 (152.391  $\rightarrow$  141.034,  $\Delta \approx -11.36$ ); highest impact on the Parabola, while other shapes gains  $\approx 25\%$  (Circle at numEx= 2: 11.071  $\rightarrow$  8.299,  $\Delta \approx -2.77$ ), suggesting that explicit memory in a small LRM preferentially improves on the ultimate goal. By contrast, Llama (dense LLM) exhibits a strong Mem $\times$ numEx interaction: memory helps at numEx= 2 (147.819  $\rightarrow$  143.836,  $\Delta \approx -3.98$ ) but can harm at numEx= 3 (142.515  $\rightarrow$  144.959,  $\Delta \approx +2.44$ ), and Parabola flips sign ( $\approx -30$  at numEx= 2 vs.  $+6.7$  at numEx= 3), implying that very large dense models possess sufficient capacity to produce valid results, as seen in the high results of semantic success, but are more sensitive to the amount of in-context examples (extra examples can induce interference). Gemma (dense LLM) displays only modest, variable responses to Mem and numEx (e.g., numEx= 2, Mem 0  $\rightarrow$  2: 153.267  $\rightarrow$  153.038,  $\Delta \approx -0.23$ ), i.e., it does not deliver robust, consistent gains from explicit memory or a single additional example.

## 4 Related Work

**Neuro-Symbolic Reasoning and Agentic Coordination and Execution** LLMs are promising for formal reasoning but often fail to reliably build and compose complex symbolic structures; self-refinement methods that feed model outputs back as corrective signals create iterative feedback loops that address some of these failures (Dziri et al.,

2023; Madaan et al., 2023; Huang and Chang, 2023). Prior agent frameworks similarly interleave symbolic plan generation with real API/simulator calls and reinforcement-style critiques to improve performance, but typically lack mechanisms for dynamic subgoal assignment and continuous state-aware review (Xiang et al., 2024; Shang et al., 2025; Yang et al., 2025; Hu et al., 2024; Yao et al., 2023; Wu et al., 2024; Gürtler et al., 2021). Framing this as an AI-systems problem, we propose a coordinated, agentic architecture where a  $\mathbb{D}a$  interacts with a simulator via executable hypotheses and a  $\mathbb{C}a$  returns structured symbolic outputs, forming a tight decomposition-execution-critique loop that enables dynamic subgoal assignment, up-to-date state feedback, and iterative self-refinement.

### Mechanism Synthesis and Data-Driven Design

One-shot neural generators map target coupler trajectories to linkage parameters and yield diverse rapid proposals. (Bai and Angeles, 2015; Lee et al., 2024) Gradient-based motion-synthesis can further optimise topology and dimensions, but is often sensitive to initialisation and penalty weighting. (Singh et al., 2024) Large collections (e.g., LINKS, ASME) provide massive static corpora for retrieval or one-shot learning. (nob, 2022; Nobari et al., 2024; Nurizada et al., 2025; Venkataraman et al., 2018; Martín-Martín et al., 2018). By contrast, our dual-agent pipeline iteratively generates candidates and synthesises symbolic and numeric critiques to steer search without relying on one-shot proposals, brittle penalty tuning, or fixed databases.

## 5 Conclusion

In this work, we introduced a dual-agent LLM-based reasoning method for mechanism synthesis, which reasons at a linguistic/symbolic level to deliver geometrical and dynamic outcomes. The method maps NL specifications to abstract properties via supporting equations, generates and parameterises simulation code, and uses SR together with distance functions to produce feedback anchors, closing an actionable refinement loop at the symbolic layer. The proposed approach proved to be effective and convergent in the context of planar mechanisms. We further introduced the MSynth benchmark. Ablations show the  $\mathbb{C}a$ 's feedback is the most transformative component, yielding up to a 90% reduction in distance. We further show that symbolic regression prompts unlock mechanistic insights in sufficiently large architectures or LRM.

## 6 Limitations

While the proposed method demonstrated strong empirical gains across all models, further investigation is required to address the causal factors behind the differences in performance across different models. Despite the fact that all LLMs exhibited chamfer gains, their underlying LLM characteristics, particularly their model size and training regimen (e.g. Qwen’s step-by-step reasoning training prior to producing its final answer), play a role. Large-capacity LLMs (Llama) or LRM (Qwen) effectively exploit symbolic equation prompts, whereas smaller models (Gemma) deliver more timid results. Finally, our experiments focus exclusively on fitting 2D geometric primitives (lines, circles, ellipses, parabolas, NACA airfoils), leaving their effectiveness in high-dimensional design spaces as a future objective.

## 7 Ethical Statement

This work explores AI-driven mechanisms to automate the systematic design of mechanism synthesis. While the work demonstrates this as a promising research direction, the proposed method is exploratory and should not be applied at this stage as a substitute for manual engineering design. Further investigation is required to critically understand the limitations of the proposed method when dialoguing with more complex mechanism synthesis scenarios.

## 8 Acknowledgements

This work was funded by the Honda Research Institute Europe GmbH (HRI) through the Mechanic project.

## References

2022. *LINKS: A Dataset of a Hundred Million Planar Linkage Mechanisms for Data-Driven Kinematic Design*, volume Volume 3A: 48th Design Automation Conference (DAC) of *International Design Engineering Technical Conferences and Computers and Information in Engineering Conference*. V03AT03A013.

Ira H Abbott and Albert E Von Doenhoff. 2012. *Theory of wing sections: including a summary of airfoil data*. Courier Corporation.

Shaoping Bai and Jorge Angeles. 2015. *Coupler-curve synthesis of four-bar linkages via a novel formulation*. *Mechanism and Machine Theory*, 94:177–187.

Vineet Bhat, Ali Umut Kaypak, Prashanth Krishnamurthy, Ramesh Karri, and Farshad Khorrami. 2024.

Grounding llms for robot task planning using closed-loop state feedback. *Preprint*, arXiv:2402.08546.

Miles Cranmer. 2023. *Interpretable machine learning for science with pysr and symbolicregression.jl*. *Preprint*, arXiv:2305.01582. This work is licensed under the Apache-2.0 license <https://github.com/MilesCranmer/PySR/blob/master/LICENSE>.

Richardos Drakoulis. 2023. Iterative closest point. <https://github.com/richardos/icp>. Accessed: 2025-05-19.

Nouha Dziri, Ximing Lu, Melanie Sclar, Xiang Lorraine Li, Liwei Jiang, Bill Yuchen Lin, Sean Welleck, Peter West, Chandra Bhagavatula, Ronan Le Bras, Jena D. Hwang, Soumya Sanyal, Xiang Ren, Allyson Ettinger, Zaid Harchaoui, and Yejin Choi. 2023. *Faith and fate: Limits of transformers on compositionality*. In *Thirty-seventh Conference on Neural Information Processing Systems*.

Hugo Farajallah. 2024. pylinkage: Python linkage builder and optimizer. <https://github.com/HugoFara/pylinkage>. GitHub repository (v0.6.0, released Oct 2 2024; accessed 2025-05-08); This work is licensed under the MIT License <https://github.com/HugoFara/pylinkage/blob/main/LICENSE>.

Daocheng Fu, Wenjie Lei, Licheng Wen, Pinlong Cai, Song Mao, Min Dou, Botian Shi, and Yu Qiao. 2024. *Limsim++: A closed-loop platform for deploying multimodal llms in autonomous driving*. *Preprint*, arXiv:2402.01246.

V. García-Marina, I. Fernández de Bustos, G. Urkullu, and R. Ansola. 2020. *Optimum dimensional synthesis of planar mechanisms with geometric constraints*. *Meccanica*, 55(11):2135–2158.

Nico Gürtler, Dieter Büchler, and Georg Martius. 2021. Hierarchical reinforcement learning with timed subgoals. *Advances in Neural Information Processing Systems*, 34.

Mengkang Hu, Tianxing Chen, Qiguang Chen, Yao Mu, Wenqi Shao, and Ping Luo. 2024. *Hiagent: Hierarchical working memory management for solving long-horizon agent tasks with large language model*. *Preprint*, arXiv:2408.09559.

Jie Huang and Kevin Chen-Chuan Chang. 2023. *Towards reasoning in large language models: A survey*. In *Findings of the Association for Computational Linguistics: ACL 2023*, pages 1049–1065, Toronto, Canada. Association for Computational Linguistics.

brian ichter, Anthony Brohan, Yevgen Chebotar, Chelsea Finn, Karol Hausman, Alexander Herzog, Daniel Ho, Julian Ibarz, Alex Irpan, Eric Jang, Ryan Julian, Dmitry Kalashnikov, Sergey Levine, Yao Lu, Carolina Parada, Kanishka Rao, Pierre Sermanet, Alexander T Toshev, Vincent Vanhoucke, and 26 others. 2023. *Do as i can, not as i say: Grounding language in robotic affordances*. In *Proceedings of The 6th Conference on Robot Learning*, volume 205 of *Proceedings of Machine Learning Research*, pages 287–318. PMLR.

- E. N. Jacobs, K. E. Ward, and R. M. Pinkerton. 1933. [The characteristics of 78 related airfoil sections from tests in the variable-density wind tunnel](#). Technical Report Report No. 460, National Advisory Committee for Aeronautics (NACA).
- Sumin Lee, Jihoon Kim, and Namwoo Kang. 2024. Deep generative model-based synthesis of four-bar linkage mechanisms with target conditions. *arXiv preprint arXiv:2402.14882*.
- Feng Lu and Evangelos Milios. 1997. Robot pose estimation in unknown environments by matching 2d range scans. *Journal of Intelligent and Robotic systems*, 18:249–275.
- Aman Madaan, Niket Tandon, Prakhar Gupta, Skyler Hallinan, Luyu Gao, Sarah Wiegrefe, Uri Alon, Nouha Dziri, Shrimai Prabhunoye, Yiming Yang, Shashank Gupta, Bodhisattwa Prasad Majumder, Katherine Hermann, Sean Welleck, Amir Yazdanbakhsh, and Peter Clark. 2023. [Self-refine: Iterative refinement with self-feedback](#). In *Thirty-seventh Conference on Neural Information Processing Systems*.
- Roberto Martín-Martín, Clemens Eppner, and Oliver Brock. 2018. [The rbo dataset of articulated objects and interactions](#). *Preprint*, arXiv:1806.06465.
- Kazem Meidani, Parshin Shojaee, Chandan K. Reddy, and Amir Barati Farimani. 2024. [SNIP: Bridging mathematical symbolic and numeric realms with unified pre-training](#). In *The Twelfth International Conference on Learning Representations*.
- Uzma Nawaz, Mufti Anees ur Rahaman, and Zubair Saeed. 2025. [A review of neuro-symbolic ai integrating reasoning and learning for advanced cognitive systems](#). *Intelligent Systems with Applications*, 26:200541.
- Amin Heyrani Nobari, Akash Srivastava, Dan Gutfreund, Kai Xu, and Faez Ahmed. 2024. [Link: Learning joint representations of design and performance spaces through contrastive learning for mechanism synthesis](#). *Preprint*, arXiv:2405.20592.
- Anar Nurizada, Rohit Dhaipule, Zhijie Lyu, and Anurag Purwar. 2025. A dataset of 3m single-dof planar 4-, 6-, and 8-bar linkage mechanisms with open and closed coupler curves for machine learning-driven path synthesis. *Journal of Mechanical Design*, 147(4).
- Brenden K Petersen, Mikel Landajuela, T Nathan Mundhenk, Claudio P Santiago, Soo K Kim, and Joanne T Kim. 2021. Deep symbolic regression: Recovering mathematical expressions from data via risk-seeking policy gradients. In *Proc. of the International Conference on Learning Representations*.
- Krishan Rana, Jesse Haviland, Sourav Garg, Jad AbouChakra, Ian Reid, and Niko Suenderhauf. 2023. [Say-plan: Grounding large language models using 3d scene graphs for scalable task planning](#). In *7th Annual Conference on Robot Learning*.
- Neider Nadid Romero, Alexandre Campos, Daniel Martins, and Rodrigo S. Vieira. 2019. [A new approach for the optimal synthesis of four-bar path generator linkages](#). *SN Applied Sciences*, 1(11):1504.
- Michael Schmidt and Hod Lipson. 2009. [Distilling free-form natural laws from experimental data](#). *Science*, 324(5923):81–85.
- Yu Shang, Yu Li, Keyu Zhao, Likai Ma, Jiahe Liu, Fengli Xu, and Yong Li. 2025. [Agentsquare: Automatic LLM agent search in modular design space](#). In *The Thirteenth International Conference on Learning Representations*.
- Parshin Shojaee, Kazem Meidani, Amir Barati Farimani, and Chandan K. Reddy. 2023. [Transformer-based planning for symbolic regression](#). In *Thirty-seventh Conference on Neural Information Processing Systems*.
- Parshin Shojaee, Kazem Meidani, Shashank Gupta, Amir Barati Farimani, and Chandan K. Reddy. 2025. [LLM-SR: Scientific equation discovery via programming with large language models](#). In *The Thirteenth International Conference on Learning Representations*.
- Ramanpreet Singh, Vimal Kumar Pathak, Ashish Kumar Srivastava, Rakesh Kumar, and Abhishek Sharma. 2024. A new metaphor-less optimization algorithm for synthesis of mechanisms. *International Journal on Interactive Design and Manufacturing (IJIDeM)*, 18(4):2371–2391.
- Sebastian Sonntag, Vincent Brünjes, Janosch Luttmer, Burkhard Corves, and Arun Nagarajah. 2024. Machine learning applications for the synthesis of planar mechanisms—a comprehensive methodical literature review. In *International Design Engineering Technical Conferences and Computers and Information in Engineering Conference*, volume 88414, page V007T07A003. American Society of Mechanical Engineers.
- L. W. Tsai. 1999. Systematic enumeration of parallel manipulators. In *Parallel Kinematic Machines*, pages 33–49, London. Springer London.
- Adrian Vasiliu and Bernard Yannou. 2001. Dimensional synthesis of planar mechanisms using neural networks: application to path generator linkages. *Mechanism and Machine Theory*, 36(2):299–310.
- Abhishek Venkataraman, Brent Griffin, and Jason J. Corso. 2018. [Learning kinematic descriptions using spare: Simulated and physical articulated extendable dataset](#). *Preprint*, arXiv:1803.11147.
- Zishen Wan, Che-Kai Liu, Hanchen Yang, Chaojian Li, Haoran You, Yonggan Fu, Cheng Wan, Tushar Krishna, Yingyan Lin, and Arijit Raychowdhury. 2024. [Towards cognitive ai systems a survey and prospective on neuro-symbolic ai](#). *Preprint*, arXiv:2401.01040.
- Lirui Wang, Yiyang Ling, Zhecheng Yuan, Mohit Shridhar, Chen Bao, Yuzhe Qin, Bailin Wang, Huazhe Xu, and Xiaolong Wang. 2024. [Gensim: Generating robotic simulation tasks via large language models](#). In *The Twelfth International Conference on Learning Representations*.

Yue Wu, Yewen Fan, So Yeon Min, Shrimai Prabhunoye, Stephen Marcus McAleer, Ruslan Salakhutdinov, Yonatan Bisk, Yuanzhi Li, and Tom Mitchell. 2024. *Agentkit: Structured LLM reasoning with dynamic graphs*. In *First Conference on Language Modeling*.

Yufei Xiang, Yiqun Shen, Yeqin Zhang, and Nguyen Cam-Tu. 2024. *Retrosplex: Language agent meets of-line reinforcement learning critic*. In *Proceedings of the 2024 Conference on Empirical Methods in Natural Language Processing*, pages 4650–4666, Miami, Florida, USA. Association for Computational Linguistics.

Ke Yang, Yao Liu, Sapana Chaudhary, Rasool Fakoor, Pratik Chaudhari, George Karypis, and Huzefa Rangwala. 2025. *Agentoccam: A simple yet strong baseline for LLM-based web agents*. In *The Thirteenth International Conference on Learning Representations*.

Shunyu Yao, Jeffrey Zhao, Dian Yu, Nan Du, Izhak Shafran, Karthik Narasimhan, and Yuan Cao. 2023. *ReAct: Synergizing reasoning and acting in language models*. In *International Conference on Learning Representations (ICLR)*.

## A Appendix: Example

Figure 4 shows a materialisation of the neuro-symbolic synthesis method for planar mechanism design. (1) Designer Agent generate hypotheses, (2) simulator simulates and Critique Agent critiques and prescribe revisions, and (3) Designer Agent performs the revision then repeat.

**1. Designer Agent.** This agent takes a target specification, either an analytic curve or sampled points, together with high-level constraints such as naming conventions, plus memory of previously validated designs, and produces executable mechanism hypotheses. It translates abstract requirements into concrete structural proposals by exploring topology and parameter spaces while enforcing hard constraints. The output is an executable representation of a mechanism (topology and parameter values) expressed in the system’s canonical design language. Emphasis is on generating a diverse set of simulation-ready candidates, biasing toward promising motifs learned from memory and avoiding known dead-ends.

**2. Simulation and Critique.** Each candidate is validated in the simulation to confirm physical executability and to convert numeric behaviour into compact, interpretable summaries. The simulation produces time-series traces of the end-effector in  $R^2$ , execution diagnostics (for example, success or failure), and a symbolic surrogate, a compact analytic expression that approximates the numeric

trace. This stage gates validity by rejecting non-executable or unstable designs, and it exposes algebraic and functional motifs in the motion through the symbolic summary.

**3. Revision.** The Revision step consumes the critique entries into structured, actionable modifications. It produces a new revised synthesis hypothesis that implements those changes. The goal is to recommend minimal, high-impact edits that improve fit and robustness while reducing unnecessary complexity, using memory to prevent repeating known failures and to suggest effective design motifs.

1. The Designer proposes one or more simulation-ready mechanism hypotheses.
2. The Simulator simulates each candidate and produces numeric traces, diagnostics, and symbolic surrogates.
3. The Critic analyses.
4. The Designer ingests the directives and memory items, revises or generates new hypotheses, and the cycle repeats.

## B Appendix: Method Algorithm

In this section, we provide a detailed description of our dual-agent iterative design loop for synthesising planar mechanisms (see Algorithm 1). Starting with an initial set of parameters, the  $\mathbb{D}a$  proposes a candidate mechanism, which is then simulated on  $\mathit{Sim}$ . Successful simulations trigger a distance-metric evaluation against the target trajectory  $\mathcal{T}$ , and SR feedback. The validated design is then stored in memory. The  $\mathbb{C}a$  then assesses performance and provides feedback on how to refine the design, prompting the  $\mathbb{D}a$  to generate updated parameters for a second simulation and re-evaluation. This cycle of design, simulation, evaluation and refinement repeats until the mechanism meets the predefined convergence or performance criteria.

You are an AI specialized in designing planar mechanisms. Based on the description, generate the appropriate mechanism using python with pylinkage library and explain each component step by step.

Commands (API Documentation):  
 Crank Definition: Define a crank (circular motor).  
 A link connecting to the ground by a revolute joint that can perform a complete revolution is called a crank link.  
`crank = pl.Crank(x, y, joint0, angle, distance, name)`  
 ...

Examples:  
 Planar Mechanism Code:  
`my_linkage = pl.Linkage(joints=(crank, slider),order=(crank, slider),name="Simple four-stroke engine")`  
 ...

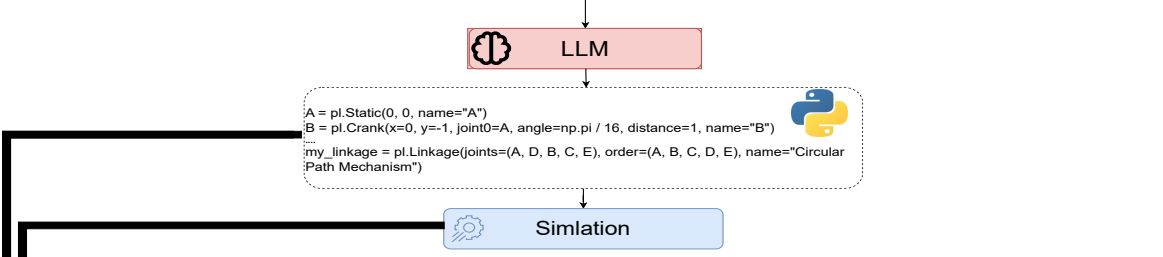
Past experiences:  
 Code:  
`A = pl.Static(0, 0, name="A")`  
`my_linkage = pl.Linkage(joints=(A, E, B, C, target), order=(A, E, B, C, target), name="Optimized Circular Path Mechanism")`  
 ...

Equation:  $(\sin(0.81/\sin(x0/(-0.06)))) - 5.07/\cos(x0)$   
 Distance: 2.730263449668435  
 Goal: minimize distance.

The model should structure the response ensuring each step has only one line of code, ensuring clarity and logical progression, strictly adhering to the commands provided.

Planar Mechanism Description:  
 Design a planar mechanism that produces a circular path.  
 Ensure that a joint follows the specified path and is designated as the 'target' The design must include a joint named 'target.' You can select which joint will serve as the target, but there must be only one target joint in the design.  
 The mechanism must pass as close as possible through all these points:  $[(-0.19, -7.05), (-0.17, -6.99), (-3.13, -3.0), (-5.96, -5.54)]$   
 Target analytical equation of the motion of the target joint is the following:  $-\sqrt{-x^*(x + 6.00)} - 6.00, \sqrt{-x^*(x + 6.00)} - 6.00$   
 Planar Mechanism Code:

1  
 Designer Agent



You are a reviewer for a mechanical designer AI agent. The following planar mechanism description:

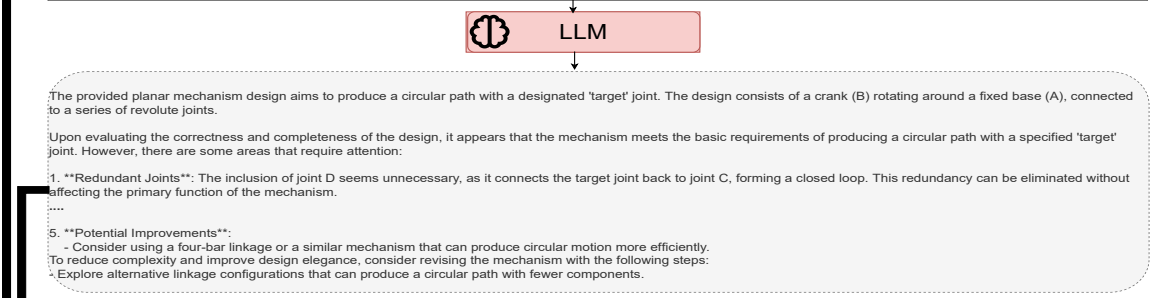
Planar Mechanism Description:  
 Design a planar mechanism that produces a circular path.  
 Ensure that a joint follows the specified path and is designated as the 'target' The design must include a joint named 'target.' You can select which joint will serve as the target, but there must be only one target joint in the design.

Simulator Output:  
 The following response was generated to fulfill the planar mechanism description

Response:  
 Your task is to evaluate the correctness, completeness, and complexity of the designed planar mechanism. Check for consistency with the problem constraints and point out any errors or improvements needed. Evaluate the complexity of the mechanism design in terms of:  
 Structural Complexity: Assess whether the design is overly complex or can be simplified while maintaining functionality.  
 Design Elegance: Consider whether the design achieves the required functionality with minimal components or steps, adhering to principles of simplicity and elegance.

Provide feedback in plain text. Point out areas where complexity could be reduced, and suggest improvements if necessary.

2  
 Critique Agent



You previously generated the following response for a planar mechanism description:

The reviewer provided the following feedback:  
 By addressing these areas, the design could be refined to improve its correctness, completeness, and overall elegance while reducing unnecessary complexity.

Past experiences:  
 Code:  
`A = pl.Static(0, 0, name="A")`  
 ...

`target = pl.Revolute(x=target_x, y=target_y, joint0=C, joint1=E, distance0=distance_targetC, distance1=6.00, name="target")`  
`my_linkage = pl.Linkage(joints=(A, E, B, C, target), order=(A, E, B, C, target), name="Optimized Circular Path Mechanism")`  
 ...

Equation:  $(\sin(0.81/\sin(x0.00/(-0.06)))) - 5.07/\cos(x0.00)$   
 Distance: 2.730263449668435  
 Goal: minimize distance.

Please revise your response to address the feedback and improve the planar mechanism.  
 The model should structure the response ensuring each step has only one line of code, ensuring clarity and logical progression, strictly adhering to the commands provided.

Planar Mechanism Code:

3  
 Revision

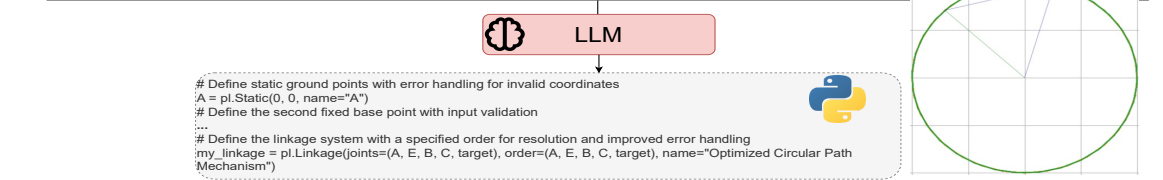


Figure 4: Neuro-symbolic closed-loop for planar mechanism synthesis: (1) Designer Agent generates executable mechanism hypotheses from the specification and memory; (2) Executor runs candidates and Critique Agent critiques and issues structured revision directives; (3) Designer Agent performs the revision, then repeats. The circle in the picture represents the path traced by the mechanism as simulated by the simulator.

---

**Algorithm 1** Iterative Planar Mechanism Design with Dual Agent, Simulation, and Evaluation

---

- 1: **Input:** Initial design parameters, Simulator on  $Sim$ , evaluation functions, target trajectory  $\mathcal{T}$
  - 2: **Output:** Optimized planar mechanism design  $\mathcal{M}(\theta)$
  - 3: **while** Design objective not met **do**
  - 4:     **Design:** Generate a new planar mechanism  $\mathcal{M}(\theta)$  using the  $\mathbb{D}a$ .
  - 5:     **First Simulation:** Simulate  $\mathcal{M}(\theta)$  on  $Sim$
  - 6:     **if** Simulation successful **then**
  - 7:         Compute distance metric  $d(\mathcal{M}(\theta), \mathcal{T})$
  - 8:         Discover SR equation
  - 9:         Store  $\mathcal{M}(\theta)$  in memory
  - 10:     **end if**
    - $\mathcal{C}a$  evaluates the mechanism and provides feedback
  - 11:     **Refinement:** Update the design strategy using feedback from the evaluation
  - 12:     **Design (Refinement):** Generate a refined mechanism  $\mathcal{M}'(\theta)$  using the updated strategy.
  - 13:     **Simulation:** Simulate the refined mechanism  $\mathcal{M}'(\theta)$  on  $Sim$
  - 14:     **if** Simulation successful **then**
  - 15:         Store  $\mathcal{M}'(\theta)$  in memory
  - 16:     **else**
  - 17:         Discard  $\mathcal{M}'(\theta)$
  - 18:     **continue** to the next iteration
  - 19:     **end if**
  - 20:     **Evaluation:**
    - Re-compute the distance metric  $d(\mathcal{M}'(\theta), \mathcal{T})$
    - Re-assess SR feedback
  - 21: **end while**
  - 22: **return** Best mechanism  $\mathcal{M}(\theta)$  or refined mechanism  $\mathcal{M}'(\theta)$  meeting design criteria
-

## C Appendix: Evaluation Metrics

**Point Set Alignment.** For a generated mechanism  $m_t$  that yields an end effector trajectory  $GeneratedPoints$ , we first perform point set registration via the ICP algorithm to establish the correspondence with the target motion profile. The algorithm aligns the generated point set with the target point set through rigid transformations, which compensates for the differences in the orientation of the coordinate systems.

**Chamfer distance** The Chamfer distance between two point sets  $P$  and  $Q$  measures their similarity by summing, for each  $p \in P$ , the distance to its nearest neighbour in  $Q$ , and doing the same from  $Q$  to  $P$ . After trajectory alignment, the mechanism’s performance is quantified using the Chamfer distance, which provides this bidirectional measure of spatial proximity between the two point sets: Formally, one common formulation is 5.

**Semantic Success Rate** We define *Semantic success* as a binary indicator of whether a generated program yields an executable. Formally, given a program  $P$ , we denote its execution in the simulator as  $T_{pred} = Sim(P)$ . Then

$$S(P) = \begin{cases} 1, & \text{if } P \text{ parses and executes without error,} \\ 0, & \text{otherwise.} \end{cases} \quad (1)$$

Implementation notes: any parse, compilation, runtime error, timeout, or early termination that prevents a simulation from being produced is treated as a failure (i.e.,  $S = 0$ ). All Python code generated by the LLM was automatically formatted with `black` to ensure a consistent style across implementations. Using `black` produces deterministic, idempotent formatting that reduces stylistic variation introduced by code generation and simplifies code inspection and review.

## D Appendix: Dataset Details

Let

$$\mathcal{S} = \left\{ \begin{aligned} &\mathcal{C}(r, x_1, y_1), \\ &\mathcal{E}(a, b, x_1, y_1), \\ &\mathcal{L}(x_1, y_1, x_2, y_2), \\ &\mathcal{P}(a, h, k), \\ &\mathcal{B}(a), \\ &\mathcal{N}(\text{series}) \end{aligned} \right\},$$

where  $r, a, b > 0$ ,  $(x_1, y_1), (x_2, y_2), (h, k) \in \mathbb{R}^2$ ,  $a \neq 0$ , and “series” ranges over the standard NACA four-digit codes  $\{2000, \dots, 3000\}$ . Each shape is defined on 6.

For each  $S \in \{\text{circle, ellipse, line, parabola, LB, NACA}\}$ , we sample 5 independent instances by drawing all shape parameters (centres, radius, semi-axes, vertex offsets, scales, chord lengths, and series codes) uniformly from their prescribed domains. We then choose  $n \in \{4\}$  uniformly at random and sample each curve at  $n$  parameter values to obtain  $\{(x_i, y_i)\}_{i=1}^n$ , which serve as the target profiles.

**Lemniscate of Bernoulli** The lemniscate of Bernoulli is a figure-eight-shaped curve defined by the quartic equation  $(x^2 + y^2)^2 = 2a^2(x^2 - y^2)$ , where the parameter  $a$  controls its overall size. It is symmetric about both axes and consists of two lobes meeting at the origin, exemplifying a simple rational algebraic curve.

**NACA Four-Digit Airfoils** Each NACA four-digit airfoil is specified by a code (e.g., “2412”) indicating maximum camber, camber position, and thickness relative to chord length. Upper and lower surface coordinates are generated by piecewise analytic formulas that ensure smooth curvature and typical aerodynamic properties, making them standard in preliminary wing design.

## E Appendix: Designer Agent ( $\mathbb{D}a$ ) Prompt

15 serves as the template for the  $\mathbb{D}a$  Prompt. It provides the structure and context that guides the  $\mathbb{D}a$  in understanding how to approach and execute design of a planar mechanism.

You are an AI specialized in designing planar mechanisms. Based on the description, generate the appropriate mechanism using Python with the `pylinkage` library and explain each component step by step.

Commands (API Documentation): `{api_doc}`

Examples:

```
# Example 1
import pylinkage as pl
crank = pl.Crank(x=0, y=0, joint0=(0, 0),
distance=1, angle=0.1, name="Crank")
slider = pl.Linear(x=2, y=0,
joint0=crank, joint1=(0, 0), joint2=(1,
```

$$d_{Chamfer}(P, Q) = \frac{\sum_{p \in P} \min_{q \in Q} \|p - q\|^2}{|P|} + \frac{\sum_{q \in Q} \min_{p \in P} \|q - p\|^2}{|Q|}$$

$$\mathcal{C}(r, x_1, y_1) = \{(x, y) \mid (x - x_1)^2 + (y - y_1)^2 = r^2\},$$

$$\mathcal{E}(a, b, x_1, y_1) = \{(x, y) \mid \frac{(x-x_1)^2}{a^2} + \frac{(y-y_1)^2}{b^2} = 1\},$$

$$\mathcal{L}(x_1, y_1, x_2, y_2) = \{(x, y) \mid y - y_1 = \frac{y_2 - y_1}{x_2 - x_1}(x - x_1)\},$$

$$\mathcal{P}(a, h, k) = \{(x, y) \mid y = a(x - h)^2 + k\},$$

$$\mathcal{B}(a) = \{(x, y) \mid (x^2 + y^2)^2 = 2a^2(x^2 - y^2)\},$$

$$\mathcal{N}(\text{series}) = \{(x, y) \mid (x, y) \text{ satisfies the standard NACA upper/lower formulas}\}.$$

`0), revolute_radius=1.5, name="target")`

`{memory}`

The analytical equation describing the motion of the target joint in the above code is given by: `{equation}` The Chamfer distance of the target equation in the above code is: `{score}`

Our goal is to minimise the distance. Therefore, the greater the distance, the more it is not following the target motion and deviating from the intended path.

Planar Mechanism Description:

`{description}`

The mechanism must pass as close as possible through all these points: `{points}`

Target analytical equation of the motion of the target joint: `{target_equation}`

Planar Mechanism Code:

### Legend for Colour Coding:

- **Brown:** Agent Role.
- **Violet:** Chain-of-Thoughts (CoT).
- **Red:** API Documentation and Mechanism Descriptions.
- **Blue:** Examples and code snippets.

- **Cyan:** Memory: previously retained knowledge.
- **Green:** Key points or constraints (e.g., points through which the mechanism must pass).
- **Orange:** Target analytical equation defining ideal behavior.
- **Purple:** Final mechanism code output.

## F Appendix: Critique Agent ( $\mathbb{C}_a$ ) Prompt

16 acts as the template for the  $\mathbb{C}_a$  Prompt. It outlines the format and expectations that help the  $\mathbb{C}_a$  deliver clear, structured, and constructive critiques to support design improvement and decision-making.

You are a reviewer for a mechanical designer AI agent.

The following planar mechanism description: `{description}`

Simulator Output: `{simulator_output}`

`{memory}`

The analytical equation describing the motion of the target joint in the above code is given by: `{equation}` The Chamfer distance of the target equation in the above code is: `{score}`

Our goal is to minimise the distance. Therefore, the greater the distance, the more it is not following the target motion and deviating from the intended

path.

The following response was generated to fulfill the planar mechanism description:

Response: {designer\_response}

Your task is to evaluate the correctness, completeness, and complexity of the designed planar mechanism.

Check for consistency with the problem constraints and point out any errors or improvements needed.

Evaluate the complexity of the mechanism design in terms of: Structural Complexity: Assess whether the design is overly complex or can be simplified while maintaining functionality.

Structural Complexity: Assess whether the design is overly complex or can be simplified while maintaining functionality.

Design Elegance: Consider whether the design achieves the required functionality with minimal components or steps, adhering to principles of simplicity and elegance.

Provide feedback in plain text. Point out areas where complexity could be reduced, and suggest improvements if necessary.

### Legend for Colour Coding:

- **Brown**: Agent's Role.
- **Red**: Planar mechanism description.
- **Orange**: Simulator output.
- **Cyan**: Memory: previously retained knowledge.
- **Purple**: Designer's response.
- **Teal**: Agent's task.

## G Appendix: Designer Agent ( $\mathbb{D}a$ ) Revision Prompt

16 serves as the template for the  $\mathbb{D}a$  Revision Prompt. It provides the structure and context that guides the  $\mathbb{D}a$  in understanding how to approach and execute design revisions effectively.

You previously generated the following response for a planar mechanism

description: {designer\_response}

The reviewer provided the following feedback: {critique\_response}

Simulator Output: {simulator\_output}

{memory}

The analytical equation describing the motion of the target joint in the above code is given by: {equation} The Chamfer distance of the target equation in the above code is: {score}

Our goal is to minimise the distance. Therefore, the greater the distance, the more it is not following the target motion and deviating from the intended path.

Please revise your response to address the feedback and improve the planar mechanism.

The model should structure the response ensuring each step has only one line of code, ensuring clarity and logical progression, strictly adhering to the commands provided.

Planar Mechanism Code:

### Appendix: Legend for Colour Coding:

- **Purple**: Previously generated response (initial planar mechanism code).
- **Magenta**: Reviewer feedback.
- **Orange**: Simulator output.
- **Cyan**: Memory: previously retained knowledge.
- **Teal**: Agent's task.

## H Appendix: Shape Complexity

In this section, we present metrics for quantifying shape complexity and compare them to our ground truth and agent-generated forms (Table 1). This concise analysis illustrates how fidelity deteriorates (or remains stable) as geometric intricacy increases. By comparing complexity scores directly across shapes, we can identify the limits of our agent's performance.

## I Appendix: Qualitative Results

Figures 5,7,9,11,13, and 15, shows the ground-truth targets, while Figures 6, 8,10, 12, 14, and 16 shows the corresponding outputs produced by our

Shape	Mean Chamfer distance
LB	$8.5654 \pm 0.1632$
Circle	$7.4564 \pm 0.5147$
Ellipse	$5.4398 \pm 0.1789$
Line	$7.1046 \pm 0.5392$
NACA	$1.1684 \pm 0.0659$
Parabola	$853.2922 \pm 6.7232$

Table 1: The mean Chamfer distances ( $\pm$  standard error) are shown for each shape category, calculated from the motion of the contours generated by the planar mechanism and the ground-truth contours.

agent. Close inspection reveals that many of the generated results closely align with their targets, accurately capturing both the global structure and fine-scale details. This strong visual correspondence highlights the effectiveness of our method in approximating the desired outputs across a range of diverse test cases.

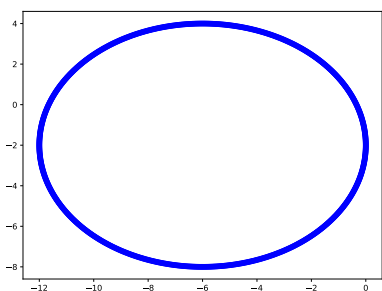


Figure 5: Ground truth Ellipse: the original target Ellipse used for evaluation.

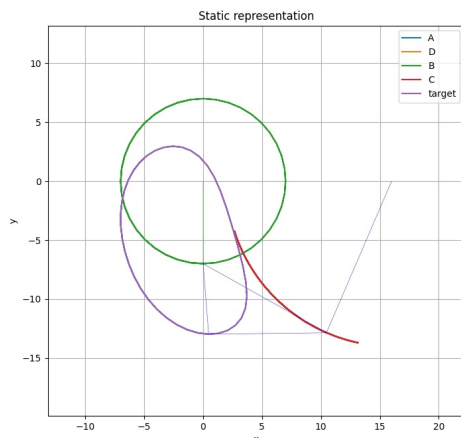


Figure 6: Generated Ellipse: the Ellipse synthesised by our agent.

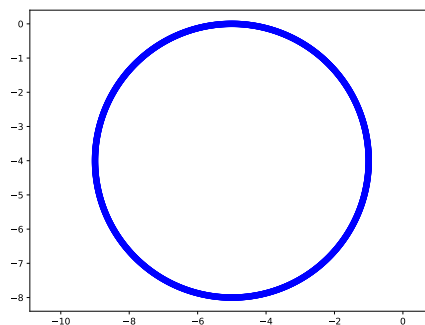


Figure 7: Ground truth Circle: the original target Circle used for evaluation.

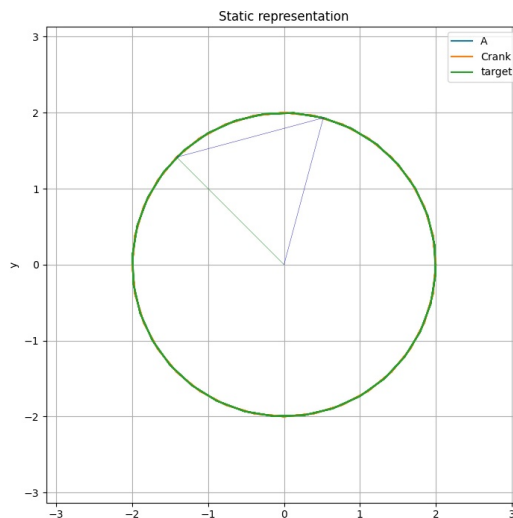


Figure 8: Generated Circle: the Circle synthesised by our agent.

## J Appendix: Hardware Configuration

We used a workstation equipped with five NVIDIA RTX 3090 graphics cards, each with 24 GB of VRAM and 72 GB of system RAM.

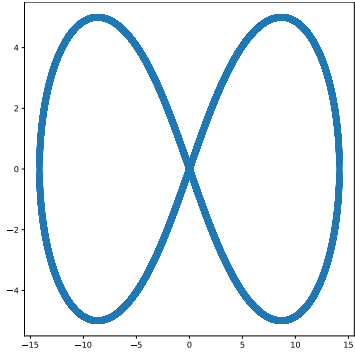


Figure 9: Ground truth LB: the original target LB used for evaluation.

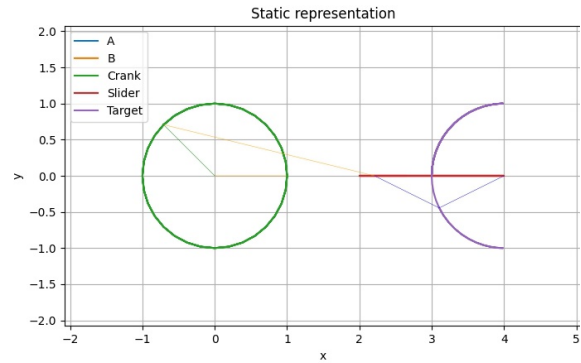


Figure 12: Generated Parabola: the Parabola synthesised by our agent.

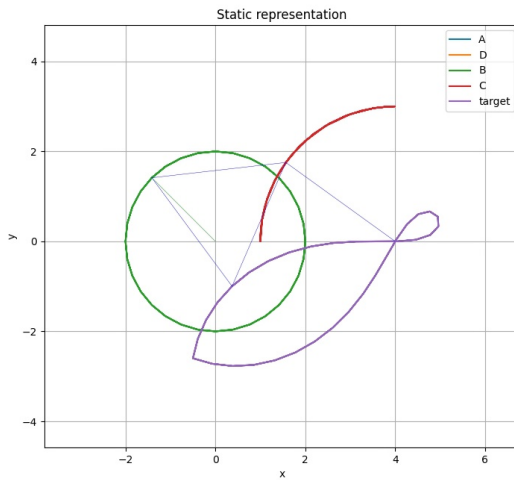


Figure 10: Generated LB: the LB synthesised by our agent.

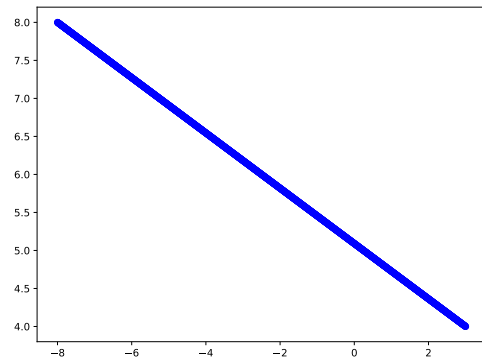


Figure 13: Ground truth Line: the original target Line used for evaluation.

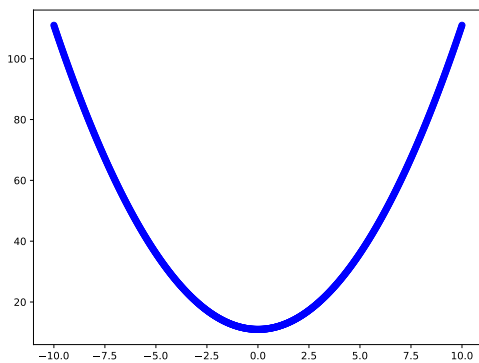


Figure 11: Ground truth Parabola: the original target Parabola used for evaluation.

mance across all six shape categories. Table 2 displays quantitative metrics, such as the average Chamfer distance and the number of convergence steps, for agent-generated outputs.

## K Appendix: Extended Quantitative Result

In this section, we present the outcomes of our complete set of experiments, summarising perfor-

Model	Shape	#Ex	Fdbk	SFB	Mem	Best chamf.	Fcham	Steps	Fstep	% Imp.	% Semantic
Gemma	LB	2	No	No	0	8.847 ± 0.493	9.078 ± 0.720	7.333 ± 2.963	7.000 ± 3.215	2.203	0.101
	LB	2	No	No	2	8.893 ± 0.851	8.893 ± 0.851	9.000 ± 4.163	5.000 ± 3.055	0.000	0.082
	LB	2	No	Yes	2	8.474 ± 1.036	8.474 ± 1.036	9.667 ± 4.055	9.667 ± 4.055	0.000	0.168
	LB	2	Yes	No	0	8.700 ± 0.375	9.043 ± 0.395	11.000 ± 2.608	6.400 ± 1.600	3.731	0.076
	LB	2	Yes	No	2	9.132 ± 0.853	9.965 ± 0.772	14.400 ± 1.720	9.600 ± 2.315	8.171	0.423
	LB	2	Yes	Yes	2	7.982 ± 0.729	9.374 ± 0.444	18.400 ± 0.245	6.200 ± 1.497	15.422	0.492
	LB	3	No	No	0	10.767 ± 0.985	11.951 ± 1.432	15.000 ± 0.577	11.000 ± 4.509	8.424	0.044
	LB	3	No	No	2	10.529 ± 0.675	10.529 ± 0.675	5.600 ± 1.720	5.600 ± 1.720	0.000	0.103
	LB	3	No	Yes	2	13.662 ± 1.679	14.552 ± 1.257	10.333 ± 4.807	5.667 ± 3.712	6.332	0.143
	LB	3	Yes	No	0	8.916 ± 0.327	10.266 ± 1.146	8.200 ± 1.744	4.400 ± 1.833	10.763	0.079
	LB	3	Yes	No	2	9.236 ± 0.561	9.612 ± 0.533	15.400 ± 1.691	6.600 ± 3.265	3.883	0.483
	LB	3	Yes	Yes	2	9.021 ± 0.656	9.763 ± 0.593	16.200 ± 2.577	6.000 ± 3.082	7.682	0.545
	Circle	2	No	No	0	8.490 ± 2.885	8.503 ± 2.874	13.750 ± 2.720	11.500 ± 2.754	1.059	0.042
	Circle	2	No	No	2	11.302 ± 3.330	11.356 ± 3.288	7.800 ± 2.010	7.400 ± 2.227	4.829	0.208
	Circle	2	No	Yes	2	8.227 ± 3.201	8.242 ± 3.189	13.750 ± 3.276	13.000 ± 3.109	1.643	0.089
	Circle	2	Yes	No	0	11.924 ± 3.486	14.248 ± 3.615	10.400 ± 2.977	5.800 ± 2.035	14.806	0.053
	Circle	2	Yes	No	2	10.899 ± 3.318	12.040 ± 3.422	15.200 ± 1.881	7.600 ± 1.939	9.651	0.527
	Circle	2	Yes	Yes	2	9.919 ± 3.420	11.597 ± 3.365	10.600 ± 2.768	1.600 ± 0.400	23.521	0.649
	Circle	3	No	No	0	11.490 ± 2.669	11.509 ± 2.654	6.000 ± 1.225	4.200 ± 1.068	0.611	0.050
	Circle	3	No	No	2	9.019 ± 2.241	11.203 ± 3.348	11.400 ± 2.768	11.000 ± 2.950	10.285	0.162
	Circle	3	No	Yes	2	6.288 ± 1.658	8.826 ± 2.147	13.600 ± 2.638	10.000 ± 2.387	20.266	0.187
	Circle	3	Yes	No	0	10.074 ± 2.260	11.837 ± 3.345	11.600 ± 2.159	8.000 ± 3.178	9.397	0.076
	Circle	3	Yes	No	2	7.351 ± 1.974	11.817 ± 3.059	13.000 ± 3.050	3.800 ± 1.356	29.604	0.595
	Circle	3	Yes	Yes	2	10.416 ± 3.413	11.744 ± 3.908	14.200 ± 2.289	3.400 ± 1.030	7.921	0.519
	Ellipse	2	No	No	0	6.677 ± 1.335	6.677 ± 1.335	9.000 ± 4.726	9.000 ± 4.726	0.000	0.029
	Ellipse	2	No	No	2	6.945 ± 2.819	6.945 ± 2.819	11.000 ± 9.000	11.000 ± 9.000	0.000	0.026
	Ellipse	2	No	Yes	2	6.568 ± 1.315	6.568 ± 1.315	3.667 ± 1.764	3.667 ± 1.764	0.000	0.176
	Ellipse	2	Yes	No	0	7.985 ± 1.375	8.928 ± 1.461	10.800 ± 1.828	7.400 ± 1.778	10.527	0.039
	Ellipse	2	Yes	No	2	6.355 ± 1.001	6.714 ± 1.133	11.600 ± 2.786	8.800 ± 2.596	4.053	0.442
	Ellipse	2	Yes	Yes	2	6.836 ± 0.991	7.348 ± 1.079	12.000 ± 2.429	10.400 ± 3.234	6.179	0.218
	Ellipse	3	No	No	0	6.722 ± 1.353	8.009 ± 1.415	6.800 ± 2.498	4.000 ± 1.265	17.586	0.211
	Ellipse	3	No	No	2	7.678 ± 1.267	7.678 ± 1.267	7.800 ± 2.709	7.800 ± 2.709	0.000	0.213
	Ellipse	3	No	Yes	2	7.372 ± 1.454	7.659 ± 1.276	7.600 ± 2.135	5.600 ± 2.272	6.428	0.371
Ellipse	3	Yes	No	0	6.900 ± 1.443	7.777 ± 1.281	12.600 ± 2.542	3.800 ± 2.332	14.609	0.121	
Ellipse	3	Yes	No	2	6.647 ± 1.244	7.445 ± 1.396	13.600 ± 3.027	6.400 ± 2.713	11.320	0.472	
Ellipse	3	Yes	Yes	2	5.552 ± 0.819	6.665 ± 1.103	12.000 ± 4.324	2.000 ± 0.775	15.391	0.394	
Line	2	No	No	0	13.640 ± 0.322	13.640 ± 0.322	11.000 ± 3.000	11.000 ± 3.000	0.000	0.002	
Line	2	No	No	2	13.643 ± 1.385	13.643 ± 1.385	10.667 ± 4.096	10.667 ± 4.096	0.000	0.136	
Line	2	No	Yes	2	12.076 ± 0.947	14.277 ± 1.254	8.500 ± 3.500	7.500 ± 2.500	14.172	0.778	
Line	2	Yes	No	0	11.150 ± 1.542	11.664 ± 1.139	10.400 ± 3.234	9.800 ± 3.484	6.050	0.032	
Line	2	Yes	No	2	10.827 ± 1.545	11.298 ± 1.214	12.200 ± 1.530	8.800 ± 2.059	6.025	0.241	
Line	2	Yes	Yes	2	10.186 ± 2.444	10.186 ± 2.444	10.600 ± 2.750	10.000 ± 2.449	0.000	0.151	
Line	3	No	No	0	8.619 ± 3.041	9.501 ± 3.392	6.750 ± 4.423	6.500 ± 4.518	6.019	0.038	
Line	3	No	No	2	11.917 ± 1.188	11.917 ± 1.188	9.000 ± 3.055	9.000 ± 3.055	0.000	0.221	
Line	3	No	Yes	2	12.071 ± 0.942	12.071 ± 0.942	4.500 ± 1.500	4.500 ± 1.500	0.000	0.319	
Line	3	Yes	No	0	9.715 ± 1.258	10.689 ± 0.921	6.800 ± 1.393	3.600 ± 1.208	10.022	0.056	
Line	3	Yes	No	2	10.043 ± 1.210	10.835 ± 1.468	10.200 ± 2.518	6.000 ± 2.387	6.166	0.552	
Line	3	Yes	Yes	2	11.035 ± 0.986	12.417 ± 1.243	14.800 ± 2.939	5.600 ± 1.806	10.570	0.371	

Model	Shape	#Ex	Fdbk	SFB	Mem	Best chamf.	Fcham	Steps	Fstep	% Imp.	% Semantic
Gemma	Naca	2	No	No	0	1.017 ± 0.436	1.017 ± 0.436	7.000 ± 1.000	7.000 ± 1.000	0.000	0.058
	Naca	2	No	No	2	1.104 ± 0.151	1.104 ± 0.151	6.333 ± 0.882	6.333 ± 0.882	0.000	0.041
	Naca	2	No	Yes	2	1.057 ± 0.416	1.057 ± 0.416	7.000 ± 0.000	7.000 ± 0.000	0.000	0.026
	Naca	2	Yes	No	0	1.082 ± 0.416	1.336 ± 0.306	12.600 ± 2.040	7.800 ± 1.715	27.086	0.078
	Naca	2	Yes	No	2	1.618 ± 0.555	1.714 ± 0.508	16.400 ± 1.364	11.800 ± 3.611	11.084	0.313
	Naca	2	Yes	Yes	2	1.074 ± 0.371	1.663 ± 0.523	12.000 ± 2.470	8.200 ± 2.709	30.463	0.522
	Naca	3	No	No	0	1.498 ± 0.499	1.628 ± 0.427	7.600 ± 2.694	4.600 ± 1.913	15.066	0.159
	Naca	3	No	No	2	1.245 ± 0.533	1.245 ± 0.533	7.000 ± 3.507	7.000 ± 3.507	0.000	0.209
	Naca	3	No	Yes	2	1.687 ± 0.518	1.883 ± 0.544	8.000 ± 1.975	5.200 ± 1.685	18.053	0.328
	Naca	3	Yes	No	0	1.347 ± 0.404	2.381 ± 0.462	6.600 ± 1.400	3.200 ± 1.428	46.926	0.146
	Naca	3	Yes	No	2	0.997 ± 0.307	2.021 ± 0.512	18.200 ± 0.860	5.000 ± 1.897	49.954	0.566
	Naca	3	Yes	Yes	2	0.796 ± 0.204	1.702 ± 0.439	13.800 ± 2.458	2.000 ± 0.548	42.740	0.854
	Parabola	2	No	No	0	869.205 ± 35.569	869.205 ± 35.569	9.500 ± 1.500	9.500 ± 1.500	0.000	0.036
		2	No	No	2	861.442 ± 28.839	861.442 ± 28.839	6.000 ± 4.000	6.000 ± 4.000	0.000	0.352
2		No	Yes	2	906.927 ± 50.681	906.927 ± 50.681	10.667 ± 3.712	10.667 ± 3.712	0.000	0.019	
2		Yes	No	0	890.160 ± 23.248	890.612 ± 23.162	13.800 ± 3.338	10.800 ± 3.513	0.052	0.023	
2		Yes	No	2	892.928 ± 23.123	897.871 ± 27.055	15.000 ± 2.168	6.000 ± 2.145	0.502	0.304	
2		Yes	Yes	2	858.509 ± 40.475	892.209 ± 23.039	12.600 ± 2.159	8.200 ± 1.744	3.784	0.300	
3		No	No	0	880.197 ± 16.446	881.267 ± 16.420	8.600 ± 1.631	5.200 ± 0.860	0.121	0.073	
3		No	No	2	897.018 ± 33.711	898.569 ± 33.387	7.600 ± 2.839	5.200 ± 2.223	0.177	0.505	
3		No	Yes	2	871.551 ± 20.077	871.551 ± 20.077	5.000 ± 3.050	5.000 ± 3.050	0.000	0.497	
3		Yes	No	0	889.653 ± 22.191	896.919 ± 24.107	11.600 ± 2.768	6.400 ± 1.288	0.788	0.072	
3		Yes	No	2	895.262 ± 24.071	905.689 ± 33.476	10.200 ± 2.818	7.200 ± 2.746	1.013	0.396	
3		Yes	Yes	2	892.568 ± 23.659	894.953 ± 22.691	10.400 ± 2.750	5.800 ± 2.354	0.278	0.513	

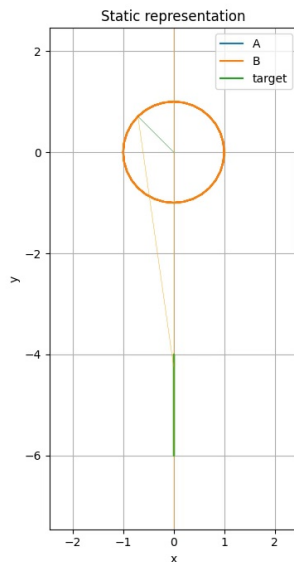


Figure 14: Generated Line: the Line synthesised by our agent.

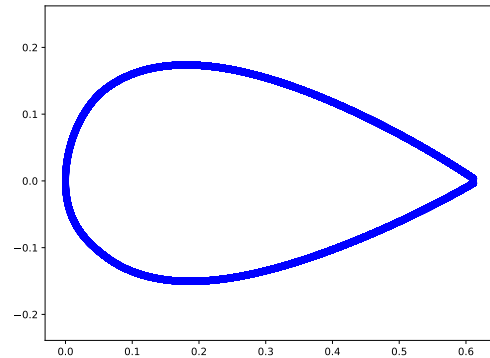


Figure 15: Ground truth NACA airfoil: the original target NACA airfoil used for evaluation.

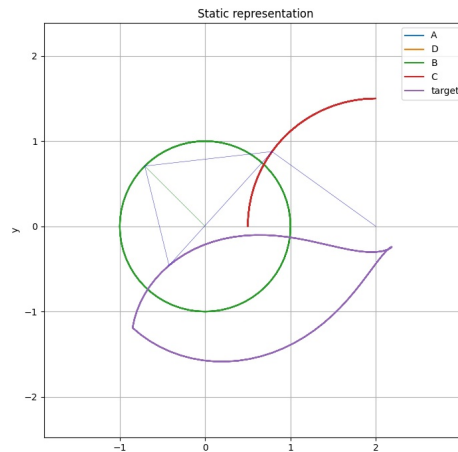


Figure 16: Generated NACA airfoil: the NACA airfoil synthesised by our agent.

Model	Shape	#Ex	Fdbk	SFB	Mem	Best chamf.	Fcham	Steps	Fstep	% Imp.	% Semantic
Llama	LB	2	No	No	0	7.415 ± 0.864	14.752 ± 2.231	14.750 ± 2.136	1.500 ± 0.289	45.126	0.231
	LB	2	No	No	2	7.730 ± 0.445	10.356 ± 1.944	3.600 ± 1.631	1.400 ± 0.245	18.120	0.786
	LB	2	No	Yes	2	8.264 ± 0.759	11.495 ± 1.094	5.800 ± 2.615	1.800 ± 0.490	25.670	0.816
	LB	2	Yes	No	0	7.029 ± 0.825	12.083 ± 1.603	10.400 ± 3.219	1.000 ± 0.000	35.867	0.375
	LB	2	Yes	No	2	7.539 ± 0.638	12.458 ± 2.201	9.250 ± 2.810	1.750 ± 0.479	34.418	0.899
	LB	2	Yes	Yes	2	7.986 ± 0.701	16.445 ± 2.855	11.000 ± 3.416	1.250 ± 0.250	45.705	0.801
	LB	3	No	No	0	7.861 ± 0.522	15.193 ± 2.333	10.600 ± 3.709	1.400 ± 0.245	43.505	0.324
	LB	3	No	No	2	10.945 ± 1.811	12.727 ± 3.415	3.750 ± 2.136	1.250 ± 0.250	8.388	0.796
	LB	3	No	Yes	2	11.656 ± 1.987	16.404 ± 2.378	4.600 ± 1.806	1.800 ± 0.583	25.118	0.576
	LB	3	Yes	No	0	6.610 ± 1.389	17.877 ± 3.803	14.667 ± 2.728	1.000 ± 0.000	57.215	0.259
	LB	3	Yes	No	2	8.017 ± 1.204	10.287 ± 1.723	4.500 ± 3.500	1.000 ± 0.000	21.837	0.969
	LB	3	Yes	Yes	2	7.337 ± 0.212	10.209 ± 1.356	17.333 ± 1.764	1.000 ± 0.000	25.852	0.855
	Circle	2	No	No	0	2.673 ± 0.714	12.537 ± 3.937	8.800 ± 3.023	2.200 ± 0.583	77.134	0.192
	Circle	2	No	No	2	11.047 ± 3.018	11.119 ± 2.962	4.000 ± 1.291	3.500 ± 1.500	1.730	0.550
	Circle	2	No	Yes	2	7.901 ± 3.435	11.478 ± 2.628	14.200 ± 2.518	6.200 ± 1.855	40.320	0.632
	Circle	2	Yes	No	0	1.466 ± 0.659	12.239 ± 3.669	17.000 ± 1.225	1.500 ± 0.289	90.609	0.238
	Circle	2	Yes	No	2	5.482 ± 2.233	12.932 ± 4.846	11.500 ± 3.069	1.750 ± 0.750	52.205	0.758
	Circle	2	Yes	Yes	2	1.930 ± 0.428	8.044 ± 3.258	17.500 ± 0.645	4.750 ± 3.119	58.285	0.676
	Circle	3	No	No	0	4.011 ± 2.143	6.372 ± 2.802	7.400 ± 3.385	2.000 ± 0.447	29.322	0.170
	Circle	3	No	No	2	7.237 ± 6.154	9.361 ± 7.705	9.667 ± 3.712	4.000 ± 3.000	22.474	0.723
	Circle	3	No	Yes	2	6.334 ± 3.305	11.281 ± 3.148	11.400 ± 2.159	2.400 ± 0.678	54.314	0.646
	Circle	3	Yes	No	0	2.181 ± 0.848	10.715 ± 4.386	7.200 ± 2.223	1.200 ± 0.200	73.424	0.387
	Circle	3	Yes	No	2	4.097 ± 2.085	11.403 ± 3.930	18.200 ± 1.562	1.400 ± 0.400	60.651	0.702
	Circle	3	Yes	Yes	2	5.660 ± 2.889	10.780 ± 3.395	11.600 ± 2.249	1.800 ± 0.800	54.820	0.826
	Ellipse	2	No	No	0	4.218 ± 0.505	7.903 ± 2.433	9.600 ± 2.542	1.600 ± 0.400	30.905	0.164
	Ellipse	2	No	No	2	4.523 ± 0.673	7.153 ± 1.232	10.200 ± 2.672	2.000 ± 0.316	34.718	0.837
	Ellipse	2	No	Yes	2	4.599 ± 0.977	6.798 ± 1.167	10.200 ± 1.828	2.400 ± 0.510	30.822	0.731
	Ellipse	2	Yes	No	0	4.113 ± 0.590	8.028 ± 1.123	14.400 ± 1.600	1.800 ± 0.374	45.818	0.252
	Ellipse	2	Yes	No	2	3.383 ± 0.391	6.356 ± 0.877	17.000 ± 1.732	2.750 ± 1.436	43.673	0.862
	Ellipse	2	Yes	Yes	2	3.371 ± 0.906	10.413 ± 5.775	12.000 ± 1.826	2.750 ± 1.750	52.252	0.737
	Ellipse	3	No	No	0	3.801 ± 0.663	8.619 ± 1.584	9.600 ± 2.713	2.000 ± 0.548	52.293	0.217
	Ellipse	3	No	No	2	5.523 ± 0.598	11.445 ± 2.579	3.800 ± 0.860	2.000 ± 0.632	43.739	0.826
	Ellipse	3	No	Yes	2	4.759 ± 0.820	7.138 ± 0.904	15.200 ± 2.267	2.600 ± 1.166	31.002	0.633
	Ellipse	3	Yes	No	0	4.048 ± 0.798	7.090 ± 1.704	4.000 ± 1.683	1.250 ± 0.250	41.283	0.303
	Ellipse	3	Yes	No	2	2.935 ± 0.621	8.870 ± 4.465	11.333 ± 1.202	2.333 ± 0.882	54.619	0.606
	Ellipse	3	Yes	Yes	2	3.429 ± 0.496	7.536 ± 2.523	8.667 ± 4.702	2.000 ± 0.577	41.305	0.785
	Line	2	No	No	0	3.479 ± 1.495	10.273 ± 1.666	12.400 ± 1.939	3.000 ± 0.894	65.454	0.113
	Line	2	No	No	2	5.999 ± 1.191	9.055 ± 1.468	9.200 ± 3.023	4.800 ± 2.577	30.440	0.541
	Line	2	No	Yes	2	5.089 ± 1.962	6.117 ± 1.809	11.000 ± 2.074	7.000 ± 2.121	18.628	0.536
	Line	2	Yes	No	0	2.935 ± 1.658	8.540 ± 2.595	8.000 ± 1.581	1.750 ± 0.750	66.011	0.138
	Line	2	Yes	No	2	2.024 ± 0.803	7.411 ± 1.205	9.750 ± 3.660	1.750 ± 0.750	62.358	0.653
	Line	2	Yes	Yes	2	4.203 ± 2.095	11.977 ± 1.247	16.000 ± 1.761	1.200 ± 0.200	66.938	0.930
	Line	3	No	No	0	1.892 ± 1.151	6.488 ± 1.696	13.000 ± 3.000	1.600 ± 0.400	70.869	0.167
	Line	3	No	No	2	2.824 ± 1.109	7.774 ± 2.180	5.000 ± 1.080	2.000 ± 0.408	47.051	0.794
	Line	3	No	Yes	2	6.741 ± 2.275	9.788 ± 1.316	9.000 ± 1.871	2.600 ± 0.980	35.589	0.661
	Line	3	Yes	No	0	0.904 ± 0.402	11.338 ± 3.167	7.250 ± 1.109	1.000 ± 0.000	89.959	0.178
	Line	3	Yes	No	2	3.281 ± 1.334	9.965 ± 3.968	14.000 ± 1.155	1.667 ± 0.333	51.229	0.675
	Line	3	Yes	Yes	2	3.090 ± 1.299	10.357 ± 2.300	14.000 ± 2.588	2.400 ± 0.600	68.001	0.758

Model	Shape	#Ex	Fdbk	SFB	Mem	Best chamf.	Fcham	Steps	Fstep	% Imp.	% Semantic
Llama	Naca	2	No	No	0	1.555 ± 0.635	2.577 ± 0.494	11.600 ± 3.043	5.400 ± 3.655	38.687	0.157
	Naca	2	No	No	2	1.247 ± 0.444	2.166 ± 0.604	4.000 ± 1.049	2.800 ± 1.114	46.449	0.624
	Naca	2	No	Yes	2	1.597 ± 0.532	1.714 ± 0.472	5.600 ± 3.187	4.800 ± 3.323	12.779	0.588
	Naca	2	Yes	No	0	0.624 ± 0.182	1.722 ± 0.494	10.400 ± 3.763	1.600 ± 0.400	57.032	0.309
	Naca	2	Yes	No	2	0.655 ± 0.209	2.469 ± 0.303	13.750 ± 1.652	1.500 ± 0.289	70.067	0.873
	Naca	2	Yes	Yes	2	0.922 ± 0.313	1.614 ± 0.701	9.667 ± 5.175	1.000 ± 0.000	29.433	0.888
	Naca	3	No	No	0	1.157 ± 0.373	2.021 ± 0.794	9.400 ± 2.542	1.400 ± 0.245	31.172	0.194
	Naca	3	No	No	2	1.315 ± 0.367	1.643 ± 0.630	4.250 ± 2.016	2.000 ± 0.707	11.631	0.828
	Naca	3	No	Yes	2	1.168 ± 0.367	2.324 ± 0.740	10.600 ± 2.337	4.600 ± 2.619	43.976	0.564
	Naca	3	Yes	No	0	0.943 ± 0.419	2.576 ± 0.817	5.750 ± 2.496	1.750 ± 0.479	66.220	0.381
	Naca	3	Yes	No	2	1.456 ± 0.571	2.291 ± 0.235	10.333 ± 4.631	2.000 ± 1.000	38.924	0.675
	Naca	3	Yes	Yes	2	1.016 ± 0.427	1.939 ± 0.472	17.500 ± 1.658	1.250 ± 0.250	49.899	0.776
	Parabola	2	No	No	0	871.702 ± 29.579	892.003 ± 24.567	13.400 ± 3.234	2.000 ± 0.548	2.319	0.224
	Parabola	2	No	No	2	872.853 ± 34.498	894.611 ± 30.983	9.800 ± 3.625	2.600 ± 0.748	2.478	0.748
	Parabola	2	No	Yes	2	851.307 ± 33.603	909.159 ± 20.136	8.000 ± 2.588	3.400 ± 2.159	6.395	0.775
	Parabola	2	Yes	No	0	866.615 ± 32.053	1125.509 ± 211.739	11.600 ± 2.379	1.400 ± 0.245	14.196	0.302
	Parabola	2	Yes	No	2	817.244 ± 83.559	900.522 ± 23.241	12.000 ± 2.775	1.200 ± 0.200	9.727	0.827
	Parabola	2	Yes	Yes	2	815.179 ± 84.612	896.679 ± 26.440	10.200 ± 2.764	1.200 ± 0.200	9.732	0.836
	Parabola	3	No	No	0	838.519 ± 33.608	879.870 ± 18.275	16.800 ± 1.985	3.200 ± 0.583	4.761	0.204
	Parabola	3	No	No	2	845.166 ± 45.083	858.242 ± 41.509	5.600 ± 1.122	2.000 ± 0.775	1.619	0.731
Parabola	3	No	Yes	2	843.717 ± 36.534	902.770 ± 49.407	11.600 ± 2.977	1.200 ± 0.200	5.900	0.787	
Parabola	3	Yes	No	0	838.254 ± 37.670	896.905 ± 23.839	14.400 ± 2.064	1.600 ± 0.400	6.597	0.294	
Parabola	3	Yes	No	2	843.277 ± 49.965	898.882 ± 26.610	11.200 ± 2.223	1.000 ± 0.000	6.205	0.820	
Parabola	3	Yes	Yes	2	848.027 ± 35.591	898.265 ± 24.218	16.600 ± 0.678	1.000 ± 0.000	5.670	0.872	

Model	Shape	#Ex	Fdbk	SFB	Mem	Best chamf.	Fcham	Steps	Fstep	% Imp.	% Semantic
Qwen	LB	2	No	No	0	8.589 ± 0.319	10.122 ± 0.512	7.400 ± 3.234	1.800 ± 0.374	13.760	0.367
	LB	2	No	No	2	8.530 ± 0.376	12.677 ± 1.963	9.600 ± 3.473	1.000 ± 0.000	26.693	0.512
	LB	2	No	Yes	2	9.129 ± 0.866	10.727 ± 1.141	11.200 ± 2.888	1.800 ± 0.374	13.545	0.611
	LB	2	Yes	No	0	8.047 ± 0.683	10.937 ± 1.311	13.200 ± 1.855	1.400 ± 0.245	25.157	0.288
	LB	2	Yes	No	2	8.763 ± 0.943	11.410 ± 1.425	6.800 ± 2.396	1.200 ± 0.200	22.070	0.471
	LB	2	Yes	Yes	2	7.830 ± 1.112	10.027 ± 0.589	14.000 ± 2.214	1.800 ± 0.374	23.076	0.467
	LB	3	No	No	0	8.460 ± 0.586	9.789 ± 0.486	11.400 ± 3.156	1.200 ± 0.200	13.869	0.381
	LB	3	No	No	2	8.075 ± 0.656	12.422 ± 2.085	15.200 ± 2.888	1.200 ± 0.200	27.637	0.349
	LB	3	No	Yes	2	7.832 ± 0.183	9.717 ± 0.465	12.000 ± 2.588	1.600 ± 0.400	18.843	0.467
	LB	3	Yes	No	0	7.291 ± 0.632	10.550 ± 1.101	10.400 ± 1.122	1.000 ± 0.000	28.501	0.310
	LB	3	Yes	No	2	6.905 ± 1.095	9.901 ± 0.439	11.400 ± 2.657	1.000 ± 0.000	28.431	0.504
	LB	3	Yes	Yes	2	7.804 ± 0.396	10.686 ± 0.758	14.400 ± 2.337	1.000 ± 0.000	25.554	0.638
	Circle	2	No	No	0	11.664 ± 3.720	11.664 ± 3.720	9.667 ± 3.844	9.667 ± 3.844	0.000	0.019
	Circle	2	No	No	2	12.950 ± 2.919	12.950 ± 2.919	12.500 ± 3.379	12.500 ± 3.379	0.000	0.019
	Circle	2	No	Yes	2	11.226 ± 3.332	11.226 ± 3.332	14.333 ± 0.333	14.333 ± 0.333	0.000	0.020
	Circle	2	Yes	No	0	10.478 ± 4.392	10.478 ± 4.392	11.200 ± 1.855	11.200 ± 1.855	0.000	0.011
	Circle	2	Yes	No	2	3.139 ± 1.309	6.518 ± 2.842	7.600 ± 2.462	7.400 ± 2.337	19.826	0.087
	Circle	2	Yes	Yes	2	5.880 ± 5.585	5.880 ± 5.585	10.667 ± 1.667	10.667 ± 1.667	0.000	0.013
	Circle	3	No	No	0	7.045 ± 4.241	8.420 ± 3.664	14.750 ± 3.276	12.250 ± 3.146	24.987	0.029
	Circle	3	No	No	2	9.131 ± 4.288	9.948 ± 3.936	12.000 ± 2.191	11.000 ± 1.817	18.175	0.059
	Circle	3	No	Yes	2	5.770 ± 5.360	5.770 ± 5.360	12.500 ± 1.500	12.500 ± 1.500	0.000	0.018
	Circle	3	Yes	No	0	5.563 ± 3.546	6.643 ± 3.277	10.200 ± 3.569	7.600 ± 3.816	19.995	0.025
	Circle	3	Yes	No	2	4.173 ± 2.654	8.734 ± 3.423	10.750 ± 2.496	5.000 ± 2.121	49.018	0.123
	Circle	3	Yes	Yes	2	6.200 ± 3.143	6.316 ± 3.087	11.600 ± 2.804	9.000 ± 1.924	19.710	0.084
	Ellipse	2	No	No	0	6.010 ± 0.958	9.740 ± 3.056	8.200 ± 2.653	1.400 ± 0.400	25.591	0.414
	Ellipse	2	No	No	2	5.166 ± 0.860	7.507 ± 1.320	12.600 ± 3.544	1.400 ± 0.400	29.698	0.562
	Ellipse	2	No	Yes	2	5.746 ± 0.928	6.984 ± 0.969	11.000 ± 3.302	1.600 ± 0.400	17.681	0.391
	Ellipse	2	Yes	No	0	4.794 ± 0.816	6.770 ± 1.179	8.800 ± 2.939	1.200 ± 0.200	24.563	0.283
	Ellipse	2	Yes	No	2	5.279 ± 0.905	8.558 ± 1.023	10.600 ± 2.839	1.000 ± 0.000	36.391	0.420
	Ellipse	2	Yes	Yes	2	4.323 ± 0.885	7.550 ± 1.321	15.200 ± 2.922	1.600 ± 0.600	38.938	0.589
	Ellipse	3	No	No	0	6.026 ± 0.949	6.664 ± 1.092	11.600 ± 4.179	1.200 ± 0.200	8.910	0.363
	Ellipse	3	No	No	2	5.958 ± 1.075	6.648 ± 1.076	5.800 ± 2.746	1.400 ± 0.245	11.515	0.524
	Ellipse	3	No	Yes	2	5.869 ± 0.854	6.886 ± 0.913	9.800 ± 3.153	1.600 ± 0.400	15.468	0.530
	Ellipse	3	Yes	No	0	4.752 ± 0.736	6.780 ± 1.049	8.800 ± 2.800	1.000 ± 0.000	29.121	0.314
	Ellipse	3	Yes	No	2	5.350 ± 1.282	9.062 ± 2.360	10.800 ± 4.030	1.000 ± 0.000	35.413	0.577
	Ellipse	3	Yes	Yes	2	4.562 ± 0.867	7.454 ± 1.236	14.000 ± 2.098	1.000 ± 0.000	35.717	0.554
	Line	2	No	No	0	7.592 ± 1.657	8.548 ± 2.231	11.000 ± 2.720	7.400 ± 3.140	7.364	0.034
	Line	2	No	No	2	7.967 ± 2.032	7.967 ± 2.032	11.000 ± 2.915	11.000 ± 2.915	0.000	0.214
	Line	2	No	Yes	2	5.757 ± 2.652	8.488 ± 2.728	8.200 ± 3.338	8.000 ± 3.162	19.165	0.027
	Line	2	Yes	No	0	7.653 ± 1.741	18.455 ± 8.155	9.800 ± 1.772	6.400 ± 1.208	34.878	0.039
	Line	2	Yes	No	2	4.236 ± 2.421	13.285 ± 3.206	11.000 ± 3.209	5.200 ± 1.356	59.558	0.466
	Line	2	Yes	Yes	2	9.153 ± 7.081	18.403 ± 8.191	9.800 ± 2.245	2.800 ± 0.800	45.798	0.639
	Line	3	No	No	0	7.081 ± 2.225	7.421 ± 2.433	9.400 ± 2.581	9.400 ± 2.581	2.468	0.046
	Line	3	No	No	2	5.088 ± 1.761	11.248 ± 2.739	11.200 ± 2.615	4.800 ± 1.281	37.601	0.590
	Line	3	No	Yes	2	15.003 ± 8.797	16.356 ± 8.538	12.200 ± 1.800	11.200 ± 2.518	10.892	0.137
	Line	3	Yes	No	0	6.913 ± 1.656	15.881 ± 8.458	11.200 ± 3.426	3.200 ± 1.020	35.913	0.058
	Line	3	Yes	No	2	8.924 ± 7.667	14.021 ± 8.520	14.800 ± 1.655	3.400 ± 0.927	41.450	0.551
	Line	3	Yes	Yes	2	2.268 ± 0.919	20.053 ± 9.575	16.200 ± 1.685	5.000 ± 2.121	83.994	0.583

Model	Shape	#Ex	Fdbk	SFB	Mem	Best chamf.	Fcham	Steps	Fstep	% Imp.	% Semantic
Qwen	Naca	2	No	No	0	1.285 ± 0.487	1.888 ± 0.356	11.600 ± 2.421	1.000 ± 0.000	41.059	0.689
	Naca	2	No	No	2	1.297 ± 0.467	1.953 ± 0.408	9.200 ± 2.154	1.000 ± 0.000	40.370	0.833
	Naca	2	No	Yes	2	1.323 ± 0.508	1.818 ± 0.472	7.600 ± 3.187	1.000 ± 0.000	32.664	0.731
	Naca	2	Yes	No	0	1.129 ± 0.476	2.320 ± 0.518	11.800 ± 2.131	1.000 ± 0.000	57.917	0.477
	Naca	2	Yes	No	2	0.887 ± 0.223	1.953 ± 0.408	14.800 ± 2.478	1.000 ± 0.000	55.968	0.553
	Naca	2	Yes	Yes	2	0.889 ± 0.263	2.677 ± 0.586	15.200 ± 2.375	1.000 ± 0.000	63.523	0.602
	Naca	3	No	No	0	1.306 ± 0.473	1.812 ± 0.472	9.600 ± 1.364	1.200 ± 0.200	32.670	0.651
	Naca	3	No	No	2	1.111 ± 0.283	1.893 ± 0.356	9.800 ± 3.216	1.000 ± 0.000	43.237	0.840
	Naca	3	No	Yes	2	1.380 ± 0.393	1.899 ± 0.407	4.600 ± 2.015	1.000 ± 0.000	31.158	0.802
	Naca	3	Yes	No	0	1.007 ± 0.382	2.130 ± 0.404	7.400 ± 1.749	1.000 ± 0.000	55.782	0.530
	Naca	3	Yes	No	2	0.876 ± 0.195	1.985 ± 0.436	13.800 ± 2.800	1.000 ± 0.000	56.462	0.742
	Naca	3	Yes	Yes	2	1.080 ± 0.401	1.980 ± 0.437	13.000 ± 2.214	1.000 ± 0.000	52.116	0.812
	Parabola	2	No	No	0	890.798 ± 24.891	896.765 ± 23.919	7.200 ± 2.746	1.200 ± 0.200	0.672	0.594
	Parabola	2	No	No	2	807.431 ± 18.711	897.205 ± 24.825	13.600 ± 2.135	1.000 ± 0.000	9.804	0.810
	Parabola	2	No	Yes	2	837.704 ± 21.792	897.545 ± 24.517	10.600 ± 3.655	1.200 ± 0.200	6.526	0.723
	Parabola	2	Yes	No	0	847.932 ± 38.709	898.009 ± 24.439	10.000 ± 2.702	1.800 ± 0.583	5.732	0.342
	Parabola	2	Yes	No	2	814.122 ± 39.460	897.491 ± 24.524	9.200 ± 2.922	1.000 ± 0.000	8.900	0.557
	Parabola	2	Yes	Yes	2	754.452 ± 54.486	899.164 ± 26.358	18.200 ± 0.860	1.200 ± 0.200	16.416	0.819
	Parabola	3	No	No	0	888.611 ± 24.141	896.433 ± 23.917	10.800 ± 2.764	1.000 ± 0.000	0.874	0.600
	Parabola	3	No	No	2	848.301 ± 41.711	897.992 ± 24.505	13.400 ± 3.219	1.200 ± 0.200	5.692	0.613
Parabola	3	No	Yes	2	895.240 ± 25.034	897.025 ± 24.547	4.200 ± 3.200	1.000 ± 0.000	0.205	0.598	
Parabola	3	Yes	No	0	884.636 ± 25.279	897.639 ± 25.247	11.200 ± 1.497	1.200 ± 0.200	1.452	0.430	
Parabola	3	Yes	No	2	818.250 ± 35.861	897.503 ± 24.680	12.600 ± 3.444	1.200 ± 0.200	8.706	0.569	
Parabola	3	Yes	Yes	2	709.656 ± 67.207	897.195 ± 23.691	15.000 ± 2.470	1.000 ± 0.000	21.299	0.840	

Table 2: Performance results across shapes and settings, where  $\pm$  denotes the standard error.